U.PORTO
FACULDADE DE CIÊNCIAS
UNIVERSIDADE DO PORTO

In vitro effects of mitochondria-targeted antioxidants in ovarian and endometrial cancer

Mariana Antunes Castelôa

Dissertação de Mestrado apresentada à
Faculdade de Ciências da Universidade do Porto em
Aplicações em Biotecnologia e Biologia Sintética

2021

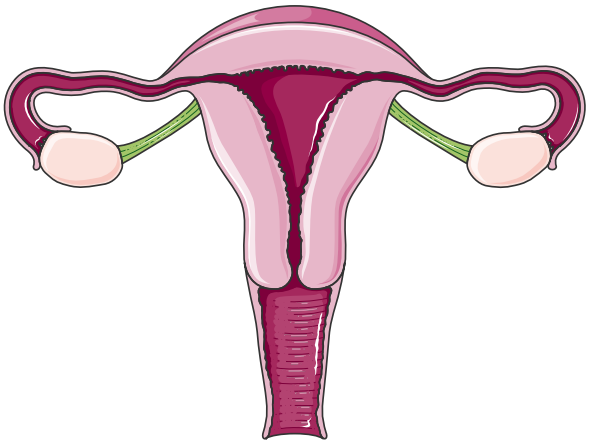

In vitro effects of mitochondria-targeted antioxidants in ovarian and endometrial cancer

Mariana Antunes Castelôa
Mestrado em Aplicações em Biotecnologia e Biologia Sintética
Departamento de Química e Bioquímica e Departamento de Biologia
2021

Orientadora
Professora Doutora Irene Rebelo, Professora Associada com Agregação do Departamento de Ciências Biológicas da Faculdade de Farmácia da Universidade do Porto

Coorientadora
Professora Doutora Fernanda Borges, Professora Associada com Agregação do Departamento de Química e Bioquímica da Faculdade de Ciências da Universidade do Porto

U.PORTO

FACULDADE DE CIÊNCIAS
UNIVERSIDADE DO PORTO

Todas as correções determinadas

pelo júri, e só essas, foram efetuadas.

O Presidente do Júri,

Porto, _____/_____/_____

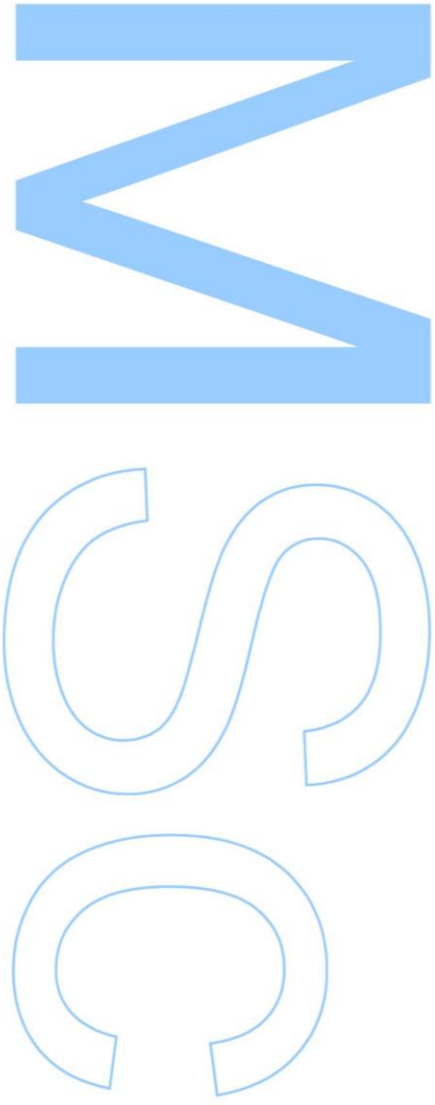

Agradecimentos

À Professora Doutora Irene Rebelo, pela oportunidade de realizar um projeto no seu laboratório novamente e pela disponibilidade sempre demonstrada ao longo do trabalho.

À Professora Doutora Fernanda Borges, pela abertura demonstrada para a realização desta parceria e pelo esclarecimento e apoio prestado sempre que necessário.

Ao Doutor Bruno Fonseca, pela confiança depositada no meu trabalho e pela transmissão de conhecimentos.

À Doutora Sofia Benfeito, pela cedência dos compostos e conhecimentos acerca dos mesmos, sem os quais este trabalho nunca poderia ter sido realizado.

À Mestre Beatriz Pinto e à Mestre Thaise Martins, por serem os meus braços direito e esquerdo, pela boa disposição contagiante em todos os momentos e por serem as melhores parceiras de laboratório que poderia pedir.

To our international students: Valentina Muzzi and Symeon Gerasimou, for allowing me to learn with them and for always bringing fun to the lab and outside of it.

Aos restantes membros do Laboratório de Bioquímica da Faculdade de Farmácia, pela disponibilidade demonstrada em esclarecer qualquer dúvida e solucionar problemas.

Aos meus amigos e meninos do bar de química, que apesar de não terem um papel direto na realização deste trabalho, foram um essencial apoio nos momentos mais complicados.

Ao Luís, por todas as ideias e conhecimentos que me permitiram evoluir neste trabalho, por me ouvir horas infindáveis e por ser o meu parceiro e pilar de apoio em todos os momentos e em todos os lugares, sem qualquer exceção.

À minha família e em particular aos meus pais, por todos os esforços ao longo destes anos e por todo o apoio que sempre me fizeram sentir.

Author's publications

- Castelôa, M.; Moreira-Pinto, B.; Benfeito, S.; Borges, F.; Fonseca, B.; Rebelo, I. *Evaluation of the effects of a TPP-based mitocan and two derivatives in ovarian and endometrial cancer cell lines.* Oral presentation at the 14th Edition of the IJUP – Young Research Meeting of the University of Porto, May 2021

- Castelôa, M.; Moreira-Pinto, B.; Benfeito, S.; Borges, F.; Fonseca, B.; Rebelo, I. *The effects of a TPP-based compound and two derivatives in ovarian and endometrial cancer cells.* Oral presentation at the 1st Edition of the BioSynBio – One-Day Meeting on Biotechnology and Synthetic Biology of FCUP, April 2021

- Castelôa, M.; Moreira-Pinto, B.; Benfeito, S.; Borges, F.; Fonseca, B.; Rebelo, I. *In vitro study of the effects of a TPP-based mitocan and two derivatives in type 1 and type 2 endometrial cancer cell lines.* Poster presentation at the University Olympiad in Biochemistry COVID-19 Special Edition, March 2021; ISBN: 978-989-33-1585-9

Resumo

O cancro do ovário e do endométrio fazem parte dos tumores do sistema reprodutor feminino com maior incidência, sendo acompanhados por uma elevada taxa de mortalidade. A sua incidência tem vindo a aumentar e o tratamento atual é inespecífico, trazendo efeitos secundários indesejados. Uma categoria de compostos com propriedades anticancerígenas que surgiu na última década são os "mitocans". Estes compostos afetam maioritariamente células tumorais através da via mitocondrial, desencadeando o processo de apoptose. Vários modelos de compostos podem ser utilizados como mitocans, desde que sejam conjugados com um catião lipofílico, tal como o trifenilfosfónio (TPP).

Neste trabalho, um antioxidante natural (ácido cafeico) foi conjugado com TPP, 4-picolina ou isoquinolina, formando 3 novos compostos (Mito6_TPP, Mito6_picol. e Mito6_isoq.) que foram testados em diferentes linhas celulares: uma linha de células tumorais da granulosa (COV434), duas linhas de células tumorais do endométrio do tipo 1 e tipo 2 (Ishikawa e Hec50co, respetivamente), e uma linha de células de fibroblastos humanos usada como controlo (HFF-1).

Os principais resultados sugerem uma diminuição na viabilidade celular (avaliada pelos ensaios de MTT e Vermelho Neutro) dependente do tempo e da concentração em todas as linhas celulares tumorais estudadas. O composto Mito6_TPP demonstrou ser ativo em concentrações mais baixas do que o Mito6_isoq. ou o Mito6_picol., porém acompanhado de efeitos citotóxicos mais evidenciados (avaliado pela medição da lactato desidrogenase). A diminuição do potencial de membrana mitocondrial apontou para a existência de apoptose. Estes resultados foram confirmados através da análise da morfologia celular (avaliada por microscopia de contraste de fase, coloração de Giemsa e coloração de Höechst). A avaliação do potencial antioxidante dos compostos foi realizada através da medição de espécies reativas de oxigénio intracelulares, que se revelaram diminuídas após tratamento. As células HFF-1 não demonstraram alterações na presença das concentrações escolhidas dos compostos. O presente estudo pretende aferir o potencial do Mito6_TPP, do Mito6_picol e do Mito6_isoq. como agentes terapêuticos contra tumores do foro ginecológico, embora seja necessária uma investigação mais profunda.

Palavras-chave: Cancro, Ovário, Endométrio, Agentes anticancerígenos, Mitocans, TPP, Antioxidantes

Abstract

Ovarian and endometrial cancer are among the most common tumors of the female reproductive system, accompanied by a high mortality rate. Its incidence has been increasing and the current treatment is nonspecific, bringing unwanted side effects. A category of compounds with anticancer properties that has emerged in the last decade are the so-called "mitocans". These compounds affect mostly tumor cells via the mitochondrial pathway, triggering the process of apoptosis. Various model compounds can be used as mitocans, provided that they are conjugated with a lipophilic cation carrier, such as triphenylphosphonium (TPP).

In this work, a natural antioxidant (caffeic acid) was conjugated with TPP, 4-picoline or isoquinoline, forming 3 new compounds (Mito6_TPP, Mito6_picol. and Mito6_isoq.) that were tested on different cell lines: a granulosa tumor cell line (COV434), two endometrial tumor cell lines type 1 and type 2 (Ishikawa and Hec50co, respectively), and a human fibroblast cell line used as control (HFF-1).

The main results suggested a time and concentration-dependent decrease in cell viability (assessed by MTT and Neutral Red assays) in all tumor cell lines studied. The compound Mito6_TPP was more active at lower concentrations than Mito6_isoq. or Mito6_picol. but was accompanied by more evident cytotoxic effects (assessed by lactate dehydrogenase measurement). The decrease in mitochondrial membrane potential points to the existence of apoptosis. These results were also confirmed through analysis of cell morphology (evaluated by phase contrast microscopy, Giemsa staining, and Höechst staining). Evaluation of the antioxidant potential of the compounds was performed by measuring intracellular reactive oxygen species, which were decreased after treatment. HFF-1 cells showed no changes in the presence of the chosen concentrations of the compounds. The present study aims to assess the potential of Mito6_TPP, Mito6_picol. and Mito6_isoq. as therapeutic agents against gynecological tumors, although further investigation is needed.

Keywords: Cancer, Ovary, Endometrium, Anticancer agents, Mitocans, TPP, Antioxidants

Index

Index of figures

Index of tables

List of abbreviations

AB-AM – Antibiotic-antimycotic

ADP – Adenosine diphosphate

ANT – Adenine nucleotide translocator

ATP – Adenosine triphosphate

Bcl-2 – B-cell lymphoma 2

CCCP – Carbonyl Cyanide m-Chlorophenylhydrazone

CI 95% – 95% confidence interval

DCF – 2',7'-Dichlorofluorescein

DCFH – 2',7'-Dichlorodihydrofluorescein

DCFH-DA – 2',7'-Dichlorodihydrofluorescein Diacetate

$DiOC_6$ – 3,3′-Dihexyloxacarbocyanine Iodide

DMEM/F12 – Dulbecco's Modified Eagle Medium/F12

DMSO – Dimethyl Sulfoxide

DPX – Dibutylphthalate Polystyrene Xylene

EC – Endometrial Cancer

EC50 – Half of maximal effective concentration

EDTA – Ethylenediamine Tetraacetic Acid

FBS – Foetal Bovine Serum

FDA – Food and Drug Administration

FF – Follicular Fluid

FSH – Follicle Stimulating Hormone

GC – Granulosa Cells

GnRH – Gonadotropin Releasing Hormone

HK – Hexokinase

INT – Iodonitrotetrazolium

LDH – Lactate Dehydrogenase

LH – Luteinizing Hormone

mtDNA – Mitochondrial DNA

MTT – Methylthiazolyldiphenyl-tetrazolium Bromide

NR – Neutral Red

NRDS – Neutral Red Destain Solution

NRM – Neutral Red Medium

OC – Ovarian Cancer

PARP – Poly(ADP-ribose)polymerase

PC – Positive Control

PBS – Phosphate Buffered Saline

PI – Protease Inhibitor Cocktail

RNS – Reactive Nitrogen Species

ROS – Reactive Oxygen Species

RPMI – Roswell Park Memorial Institute 1640

SEM – Standard Error of the Mean

TC – Theca Cells

TPP – Triphenylphosphonium

VDAC – Voltage-dependent anion channel

$\Delta\psi m$ – Mitochondrial membrane potential

Introduction

1. Female reproductive system

The female reproductive system is a complex where a variety of elaborated processes occur to allow reproduction. Together, these processes constitute the menstrual cycle. This is an intricate cycle that involves a sequence of events that start in the hypothalamus and affect the anterior pituitary, the ovary, and the endometrium. It is also possible to divide the menstrual cycle into two phases: the follicular phase and the luteal phase, both characterized by diverse events and regulated by different hormones. Between these phases, ovulation occurs and, in case the oocyte is not fertilized, the superficial layer of the endometrium degenerates originating the menstruation. As the menstrual cycle is characterized by events occurring both in the ovary and the uterus, it is possible to define the ovarian and the uterine cycles characteristics[1] (Figure 1).

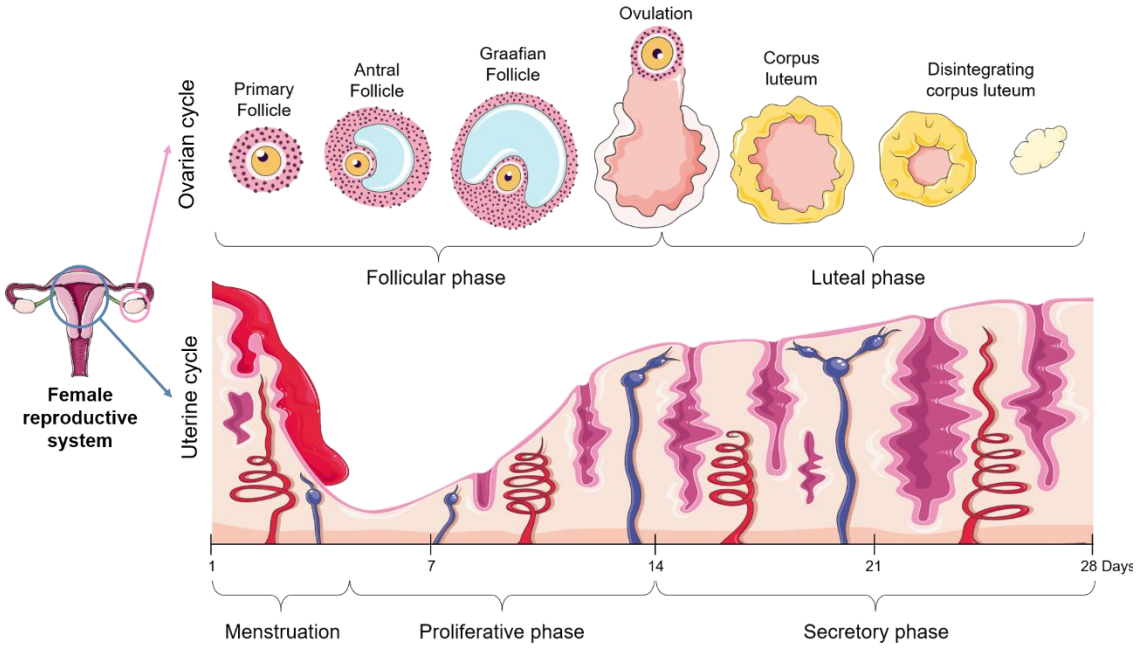

Figure 1 – Ovarian and uterine cycles of the human female menstrual cycle. The follicular phase begins with the degeneration of the endometrium (menstruation) and the development of new follicles. Then, the endometrium starts thickening (proliferative phase) while only one of the follicles starts to become dominant. At the end of this phase, ovulation occurs. The luteal phase is characterized by the formation of the *corpus luteum* that prepares the endometrium for the implantation of an embryo (secretory phase). In case of a non-pregnancy cycle, the *corpus luteum* will degenerate, initiating a new menstrual cycle[2].

The ovarian cycle is based on the development of follicles namely, folliculogenesis. These follicles are constituted by oocytes surrounded by granulosa cells (GC) that offer protection, nutrients and chemical messengers. At the beginning of the follicular phase, follicles are named primary or primordial follicles and are constituted by one oocyte surrounded by a single layer of GC. As their size increases and GC proliferate into more layers, a secondary follicle is formed. The theca cells (TC) layer and the antrum, a cavity

filled with follicular fluid (FF), are then formed and these follicles are named tertiary follicles or antral follicles. Then, the volume of FF increases and a projection of GC is formed into it, establishing the cumulus oophorous. This maturation originates a mature follicle or Graafian follicle[3] (Figure 2). The ovulation occurs when the Graafian follicle joins the ovary wall, disrupting it and setting the oocyte free. The luteal phase starts after ovulation when the remaining follicular cells originate the *corpus luteum*[1, 4] (Figure 1).

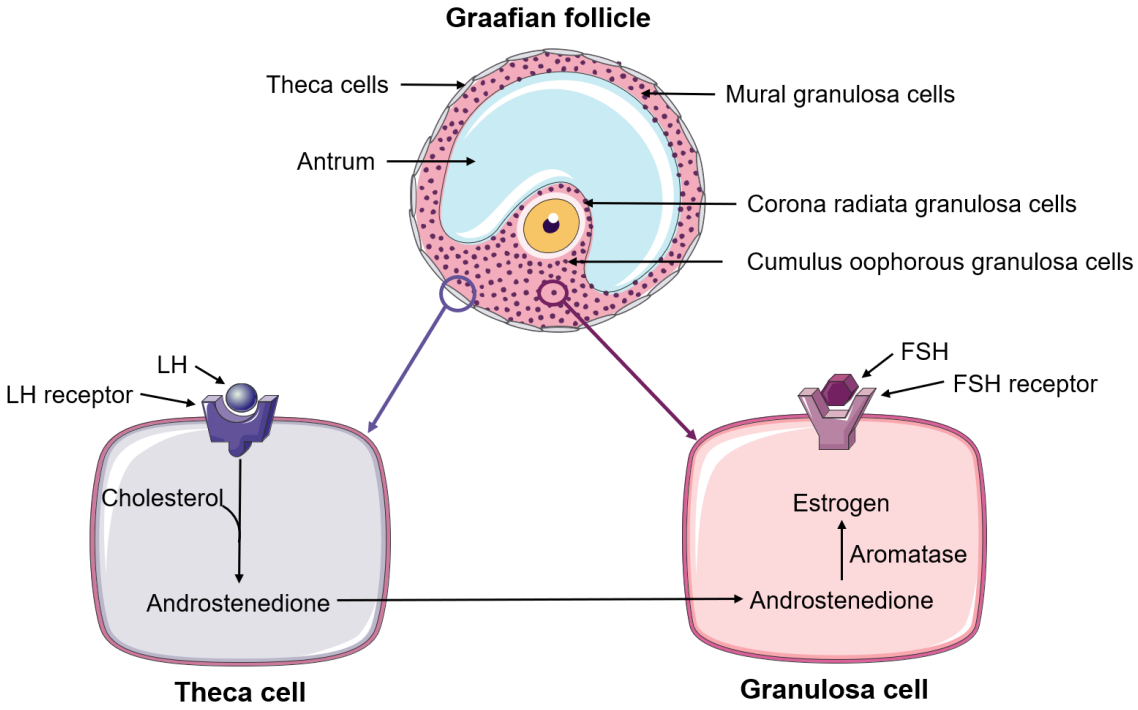

Figure 2 – Graafian follicle and estrogen production by GC. The Graafian follicle is characterized by a very large antrum, a layer of GC surrounding the oocyte (corona radiata GC), a projection of GC into the antrum (cumulus oophorous GC), a mural of GC, and a layer of TC. TC and GC interact to produce estrogen, this process starts with the LH stimulation in TC that use cholesterol to produce androstenedione which diffuses to GC, activated by FSH, to be converted by aromatase into estrogen[5].

The uterine cycle starts with menstruation, the process in which the superficial layer of the endometrium disintegrates and is removed from the uterus at the end of the luteal phase of a non-pregnancy cycle. The proliferative phase starts right after and is characterized by endometrial thickening. Then, the endometrium is prepared to receive an embryo if fertilization occurs, naming this phase as the secretory phase[6, 7] (Figure 1).

These cycles are regulated by different hormone levels and one of the main regulatory elements of these cycles is the gonadotrophin-releasing hormone (GnRH) that is produced in the hypothalamus. This hormone stimulates the production of two other hormones by the anterior pituitary: the follicle-stimulating hormone (FSH) and the luteinizing hormone (LH)[8, 9]. A small increase in the FSH levels induces the beginning of the follicular phase, stimulating the development of new follicles. Simultaneously, low levels of estrogen and progesterone promote the degeneration of the endometrium.

Stimulation of GC and TC in the developing follicles by FSH and LH, respectively, results on an increase in estrogen levels, that in turn induce thickening of the endometrium (Figure 2). A few days after, a decrease in FSH will allow only one (occasionally more) follicle to become dominant, and a peak of LH will induce ovulation. The levels of these hormones will decrease and the luteal phase will begin. In this phase, the remaining follicular cells form the *corpus luteum,* which produces progesterone that will prepare the endometrium to receive an embryo, in case fertilization occurs. Otherwise, the *corpus luteum* degenerates, and progesterone and estrogen levels drop, starting a new menstrual cycle[10] (Figure 3).

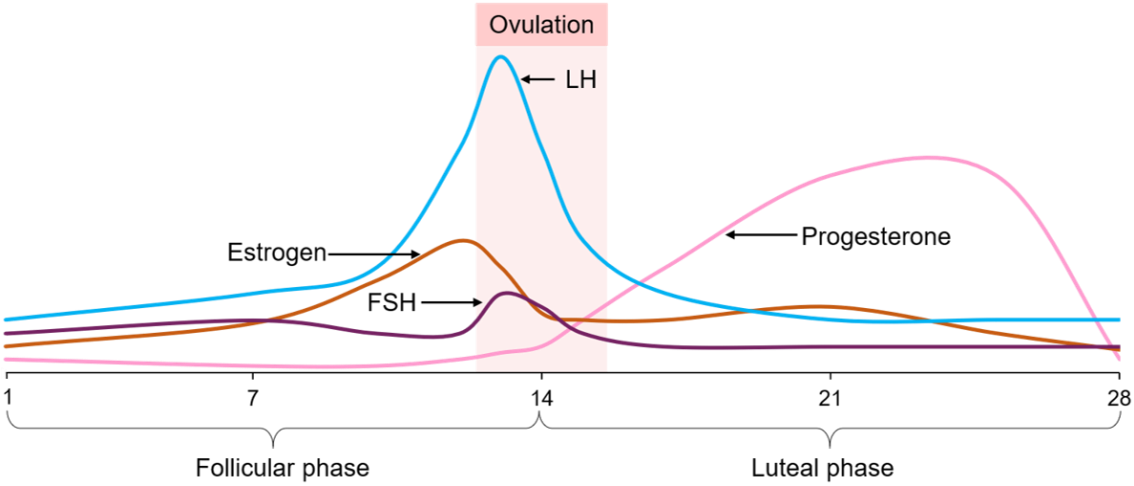

Figure 3 – Variation of the hormone levels on the human female menstrual cycle. The follicular phase is initiated by a small increase in the FSH levels. At the same time, the low levels of estrogen and progesterone induce the breakdown of the endometrium. The follicles in development will increase the production of estrogen, initiating the thickening of the endometrium and inducing a decrease in FSH which will allow only one of the follicles to become dominant. It is at the same time that a peak of LH appears and induces ovulation. The luteal phase begins when the levels of LH and FSH decrease and the *corpus luteum* is formed, producing progesterone. Progesterone allows the endometrium to receive an embryo if fertilization has occurred. Otherwise, the *corpus luteum* degenerates initiating a new menstrual cycle[8, 10].

2. Gynecological cancers

2.1. Ovarian cancer

Ovarian cancer (OC) is the third most common cancer of the female reproductive tract and the most lethal in this category, being one of the most common causes of death from cancer in women[11]. The high mortality of this pathology is associated with late detection of the tumor, and it is expected that the incidence of these tumors will increase around 40% in cases and more than 50% in deaths by 2040 compared to 2020[12] (Figure 4). It is more common in industrialized countries probably due to the fact that, in this particular case, women usually have fewer children than in less developed countries and it is estimated that each pregnancy lowers the risk of OC by a third[13].

These tumors can be sporadic in 90% of the patients, but 10% of them have inherited syndromes, such as breast-ovarian cancer syndrome, characterized by mutations in the

BRCA1 and *BRCA2* tumor suppressor genes[14]. Other risk factors include advanced age, infertility, obesity, hormone replacement therapy, among others[13]. Interrupting ovulation by using oral contraception has been shown to decrease the intrinsic risk for OC, but in suspected cases of, for example, *BRCA* mutations, surgical removal of the ovaries is also performed[15]. The most common symptoms include: increased abdominal size, fatigue and abdominal and pelvic pain, although, in 5% of the cases, there are no symptoms, delaying the diagnosis[16]. These statistics show the importance of developing new and more effective therapies able to combat this disease to prevent the estimated increase of cases and deaths. However, these tumors have different characteristics that must be considered when studying these pathologies.

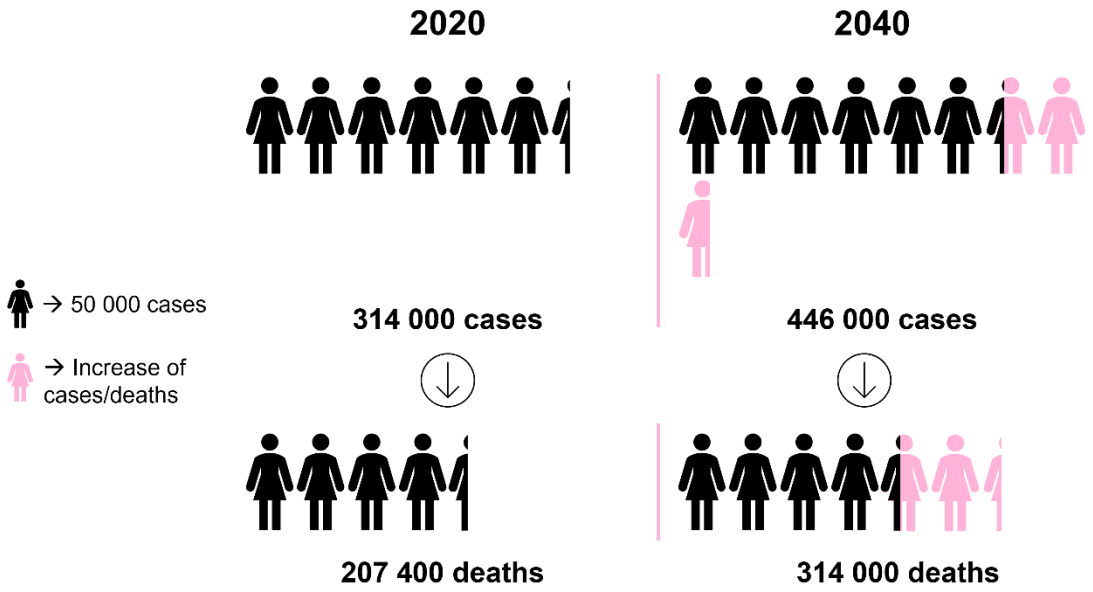

Figure 4 – Estimation of the increase of cases and deaths caused by ovarian cancer worldwide by 2040. The incidence of this pathology is expected to increase around 40% in cases and more than 50% in deaths by 2040 (Statistics from the International Agency for Research on Cancer [12]).

Ovarian tumors can be classified in three different ways, depending on where they are allocated: surface epithelial-stromal tumors, germ cell tumors, and sexual cord-stromal tumors. The most common are those that arise on the surface epithelium, completing 60% of all ovarian tumors. They tend to appear with increasing age, being more incident in women aged 60-70 years. Germ cell tumors consist of 20%-25% of ovarian tumors and occur more frequently in younger women aged 15-19 years. Sexual cord-stromal tumors comprise only 5%-10% of all ovarian tumors and appear predominantly in older and postmenopausal women[17].

In particular, GC tumors are the most common tumor of the sexual cord and, while is it predominant in older adult women, it also has a juvenile form that can affect younger women and children[14]. Most of these tumors, around 90%, are restricted to the ovary,

presenting a good prognosis. However, the reappearance of the tumor a few years after surgery usually happens and tends to be fatal. Although it is a rare tumor with a good prognosis if detected early, this is the most common estrogen-producing tumor. High estrogen production by these tumors is associated with endometrial hyperplasia and, consequently, with cancer, being estimated that the GC tumors can be associated with endometrial tumors in up to 25% of the cases[18].

To study tumors *in vitro*, it is possible to use some cell culture models that have become an essential tool to reveal molecular mechanisms and to assess the safety and efficacy of potentially therapeutic drugs. This type of screening happens before the preclinical animal studies and is crucial to determine if the molecule has the potential to be used as a therapy[19]. In this case, it is possible to use GC tumor cell lines, such as KGN and COV434. In particular, COV434 is an immortalized human granulosa cell line established in 1984 from a 27-year-old female primary tumor. These cells can also be used in studies on the development of the follicles due to some characteristics that they maintain compared to healthy GC, such as the presence of the FSH receptor and aromatase that allow the synthesis of estradiol and the ability to undergo apoptosis. However, they do not possess LH receptor[20].

2.2. Endometrial cancer

Although it is not as deathly as OC, endometrial cancer (EC) is nowadays a problematic gynecological disease that affects women worldwide and especially in developed countries, being estimated to be the second most common gynecological cancer and the fourth most prominent cause of death among these diseases[11, 21]. It is also projected that the incidence level of this cancer will increase drastically, allowing it to grow around 50% by 2040 compared to 2020[12] (Figure 5).

This increase in the incidence level of EC can be attributed to some risk factors, including obesity, hypertension, diabetes, and hyperestrogenism due to therapy or pathologies, such as a granulosa cell tumor[18]. However, about 5% of the EC cases can have genetic causes[22, 23]. Just like the OC, the decrease of exposure to risk factors and the intake of oral contraceptives can lower the risk of developing EC[24]. The most prominent symptoms include postmenopausal bleeding, fatigue, abnormal vaginal discharge and irregular menstrual cycles that usually occur in later stages of the desease[25]. Like OC, these data clarify the urge for new innovative therapies that can combat this pathology.

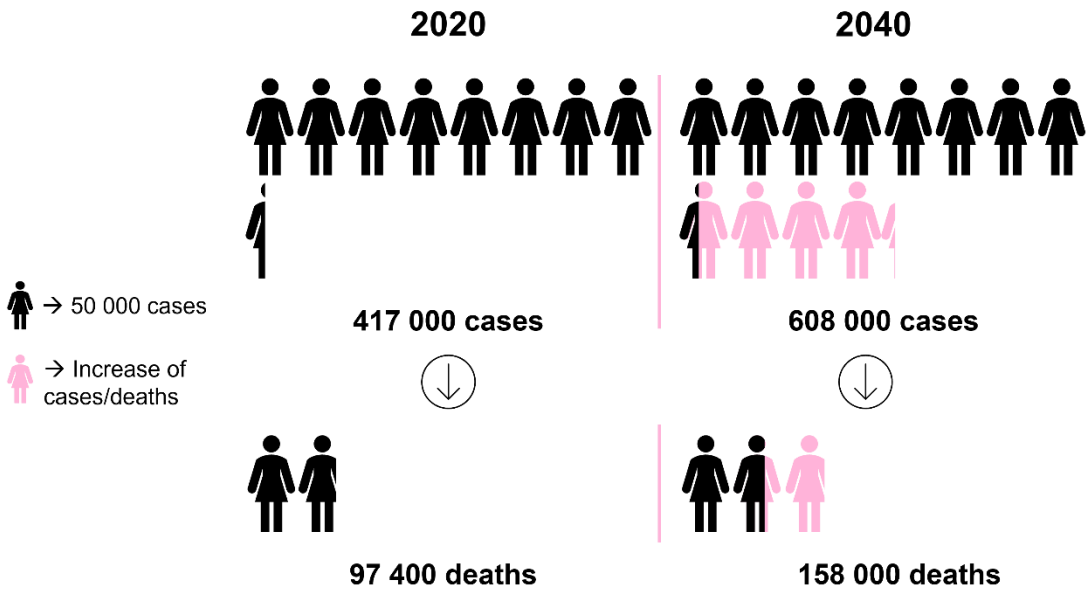

Figure 5 – Estimation of the increase of cases and deaths caused by endometrial cancer worldwide by 2040. The incidence of this pathology is expected to increase around 50% either in cases or deaths by 2040 (Statistics from the International Agency for Research on Cancer [12]).

EC can be categorized into two categories: type 1 and type 2. These types show differences in aggressiveness and response to treatment, implying differences in prognosis. Type 1 occurs most often in postmenopausal and anovulatory women and accounts for approximately 80% of all EC cases. Clinically, they present low-grade features, implying a good prognosis, since the cells are usually well-differentiated and the surrounding tissue appears to be hyperplastic. Type 2 occurs predominantly in postmenopausal women and consists of poorly differentiated cells, often associated with nearby endometrial atrophy, implying higher-grade cancer and a worse prognosis that requires a more aggressive treatment[26, 27]. Another characteristic that allows differentiation of these two types of EC is the dependence of estrogen to grow: while type 1 tumors are estrogen-dependent, type 2 are estrogen-independent (Table 1).

Table 1 – Comparison of the characteristics of type 1 and type 2 endometrial cancer.

Characteristic	Type 1	Type 2
Patient Occurrence	Postmenopausal/Anovulatory	Postmenopausal
Cell Differentiation	Well differentiated	Poorly differentiated
Surrounding Tissue	Hyperplastic	Atrophic
Prognosis	Good	Bad
Estrogen Dependency	Dependent	Non-dependent

In order to study EC *in vitro*, it is necessary to use cell models that well represent both type 1 and type 2 tumors. The Ishikawa cell line was established from an endometrial adenocarcinoma patient and expresses both estrogen and progesterone receptors, making this cell line a suitable model for type 1 EC[28, 29]. Hec50co cell line consists of

poorly differentiated endometrial tumor cells isolated from a patient with advanced disease and expresses only residual levels of estrogen receptors, allowing this cell line to be used as a model for type 2 endometrial tumors[30].

3. Anticancer agents

Recently, the pharmaceutical industry has faced certain challenges due to the increase of expense in drug development and the decrease in effective drugs obtained, compromising the patients' treatments. Nevertheless, new advances in science and technology have improved the drug development process, such as structure-based drug design, combinatorial and parallel chemistry, and high-throughput screening[31]. Specifically, there is a great need to develop new anticancer drugs and systems to deliver them that are capable of producing the desired effects without the aggressive side effects that currently used drugs produce.

Depending on their mechanism of action, anticancer agents can be classified into two broad categories: cytotoxic agents and targeted agents. Cytotoxic agents induce death in cells that reproduce at a high rate like tumor cells, as they directly target mitosis and DNA replication pathways, implying that healthy cells will also be affected to control the spread of cancer. Some examples of cytotoxic drugs include DNA alkylating agents, inhibitors of topoisomerase, antimetabolites and microtubule-active agents[32]. Targeted agents attack specific molecular targets important for tumor progression, blocking its growth and affecting less healthy cells. Targeted drugs attack molecular targets such as the tyrosine kinase, the heat shock protein 90 and proteins involved in the apoptosis process[32] (Table 2). Nowadays, there are many more cytotoxic agents than targeted agents approved, for example, the treatment for OC only had 2 targeted drugs available for therapy, while there were 10 cytotoxic drugs approved by the Food and Drug Administration (FDA) in 2017[33]. The aim at the moment is to try to reverse this ratio and increase the number of available targeted agents.

Table 2 – Comparison of the characteristics of cytotoxic and targeted anticancer drugs.

Characteristic	Cytotoxic drugs	Targeted drugs
Mechanism of action	Disruption of DNA or mitotic function	Specific targets in tumor cells
Selectivity dependency	Rate of cell division	Characteristics of tumor cells
Normal cells affected	Yes	Rarely
Examples	DNA alkylating agents, inhibitors of topoisomerase, antimetabolites, microtubule-active agents	Selective tyrosine kinase inhibitors, heat shock protein 90 inhibitors, inhibitors of apoptosis protein antagonists

Some specific compounds have been used to try to increase the effectiveness of currently used drugs, and try to transform some currently used cytotoxic drugs into targeted drugs. In particular, pyridine derivatives, such as 4-methylpyridine or 4-picoline (Figure 6a), are lipophilic compounds that are already used by the pharmaceutical industry as antimicrobials, antivirals, antidiabetics and anticancer agents[34]. Some studies suggest that the conjugation of these motifs to current anticancer agents can improve their efficacy. In 2018, Rahman, F. U. *et al.* showed that Pt(II)(hydrazone) complexes where a 4-picoline moiety was added presented higher anticancer effects than the original complexes, showing a decrease in cell viability and migration and inducing apoptosis in liver and lung cancer cell lines[35]. Previously, the same group also found that complexes of cisplatin and picoline showed higher cytotoxicity than cisplatin alone and induced apoptotic genes expression as well as Poly(ADP-ribose)polymerase (PARP) cleavage in breast, liver, lung, colon, and cervical cancer cell lines[36].

Another example is the isoquinoline derivatives (Figure 6b) that have antibacterial, analgesic and immunoregulatory properties, among others. It is also known that these lipophilic compounds can inhibit certain cancer-associated enzymes, such as inosine 5'-monophosphate dehydrogenase (expressed in prostate tumors), P-glycoprotein (associated with drug resistance), and cyclin-dependent kinase 4 (suppresses tumor suppression mechanisms), having an interesting antitumor potential[37]. A study that proves its anticancer potential was conducted by Ding, D. *et al.* in 2016, which found that isoquinoline-based compounds showed high cytotoxicity specifically in cancer cell lines and induced apoptosis[38].

Figure 6 – Examples of cations used to improve the efficacy of anticancer drugs. (a) 4-Methylpyridinium or 4-picolinium; (b) Isoquinolinium.

Even the same type of tumor can have different characteristics in different patients, due to different expression levels and mutations in various genes. This implies that a targeted drug that affects only one single gene or pathway might be effective for one patient, but not for others[39]. This is one of the disadvantages of some targeted drugs. Consequently, it is necessary to find a consistent target that can be a base for effective treatment in various tumors and patients.

4. Mitochondria as a therapeutic target

One target that has shown potential to be attacked by targeted drugs is the mitochondria. Mitochondria are the organelles responsible for producing ATP through respiration but contain a variety of other functions, such as regulating the cell proliferation and death processes, among others[40]. One of the reasons they are a good potential target is the fact that they are functional in tumor cells, but have different characteristics from healthy cells, such as an aberrant metabolism[41]. They are also essential for cell survival and possess proteins that are essential to promote apoptosis[42, 43]. Tumor cells are considered to suffer the Warburg effect that consists of a modification in the cellular metabolism, where the cells prefer to use fermentation instead of aerobic respiration, even in the presence of oxygen[44]. Therefore, their main source of energy is glycolysis, but it is now known that several functions in the mitochondria, such as oxidative phosphorylation, redox control, calcium homeostasis, regulation of transcription and cell death control, also play a key role in cancer cells[45]. Consequently, tumor cells take advantage of glycolysis and oxidative phosphorylation as both processes are essential for their growth[46]. Thus, researchers have lately focused on developing new agents that can target tumor cells' mitochondria in different locations, such as the inner membrane or the mitochondrial DNA (mtDNA) and induce cell death (Figure 7). These substantially promising anticancer agents who have selectivity for tumor cells' mitochondria are usually called mitocans, a mix between mitochondria and cancer[47].

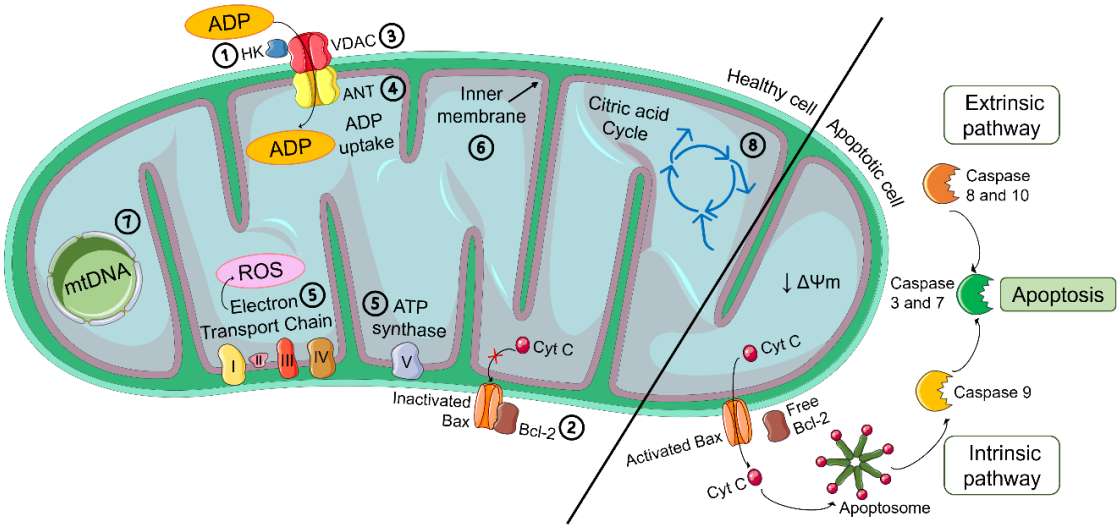

Figure 7 – Mitocans possible targets in the mitochondria and the process of apoptosis they can trigger. Left: Different targets that mitocans can use to induce cell death, identified by class: Class 1: Hexokinase inhibitors; Class 2: Bcl-2 family inhibitors; Class 3: Thiol redox inhibitors; Class 4: Adenine nucleotide translocase targeting drugs; Class 5: Drugs that attack the electron transport chain and ATP synthase; Class 6: Inner membrane-targeting drugs; Class 7: Drugs targeting the citric acid cycle; Class 8: Drugs targeting the transcription and translation of mtDNA. **Right:** Extrinsic and intrinsic apoptotic pathways. In the intrinsic pathway, a stimulus induces the Bcl-2 protein to release the Bcl-2 associated X protein (Bax), activating it. This will trigger membrane depolarization, implying a decrease in the mitochondrial membrane potential (Δψm), that will release of cytochrome C (Cyt C). Cyt C will stimulate the assembly of the apoptosome that will activate caspase 9, and consequently caspase 3 and 7, culminating in apoptosis. In the extrinsic pathway, caspases 8 and 10 will be activated by external factors and cleave the caspase 3 and 7, culminating in apoptosis. ADP: Adenosine diphosphate; ATP: Adenosine triphosphate; ANT: Adenine nucleotide translocator; HK: Hexokinase; VDAC: Voltage-dependent anion channel. Adapted from Paulo, J. O. [48-51].

There is a very widely used moiety to target the mitochondria, it is the triphenylphosphonium (TPP) cation. It is a lipophilic cation that can penetrate the mitochondrial membrane and accumulate in its matrix due to its negative membrane potential[52, 53]. In fact, this cation is selective between tumor cells and healthy cells since the mitochondrial membrane potential of tumor cells is around 60mV higher than normal cells, increasing the cations' tendency to accumulate in this type of cells instead of normal cells[54]. TPP has shown cytotoxic activity on its own, and can therefore act as a mitocan without being conjugated with another compound. However, it is most used conjugated with another scaffold to improve their targeting to the mitochondria and its pharmacological effect[49]. It can be linked to natural products, antioxidants, commercialized drugs, small cytotoxic molecules, thermo-sensitive agents, photosensitizers, and enzyme inhibitors, among other types of compounds, making the TPP moiety helpful to combat various pathologies besides cancer (Figure 8)[54, 55].

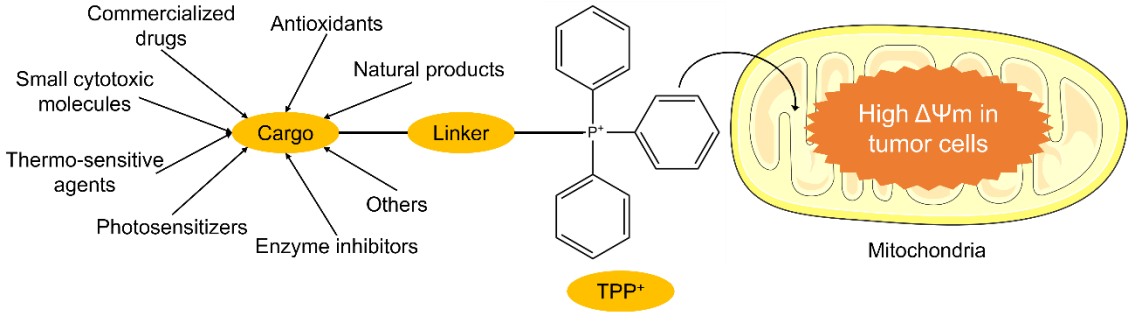

Figure 8 – Design of a TPP-based mitocan. Various types of compounds can be linked to a TPP cation, that has the ability to accumulate in the mitochondrial matrix, especially in tumor cells that have higher mitochondrial membrane potential (Δψm) than normal cells**.** Adapted from Wang, J. *et al.*[54].

Several studies have recently shown targeting and pharmacological improvements in the compounds with the addition of the TPP moiety. Sandoval-Acuña, C. *et al.* concluded in 2016 that several decyl-polyhydroxybenzoates conjugated with the TPP cation for the mitochondrial target were cytotoxic and inhibited the metastatic capacity at sublethal concentrations in various breast cancer cell lines, independently of their hormone receptors[56]. Recently, Ma, L. *et al.* studied the anticancer effect of several ginsenosides incorporated with TPP moiety to improve the compounds' efficacy and selectivity, finding that the complexes had higher antiproliferative effects and induced apoptosis by increasing ROS levels and decreasing mitochondrial membrane potential (Δψm)[57].

5. Antioxidants

It is well established that ROS are used by tumor cells to stimulate growth and survival, being acknowledged their increased presence in various tumors[58]. However, excessive levels of ROS induced by the presence of the inflammatory process can be toxic to the cell, causing irreparable damage and leading to self-destruction. Therefore, tumor cells

need to control ROS levels and, to combat its excess, tumor cells produce equally high levels of antioxidants that will capture additional ROS and prevent oxidative stress[59]. Nevertheless, if antioxidant levels are higher than ROS levels, the tumor cell will not have the necessary stimulus to continue its growth and progression and will begin to degenerate (Figure 9)[60].

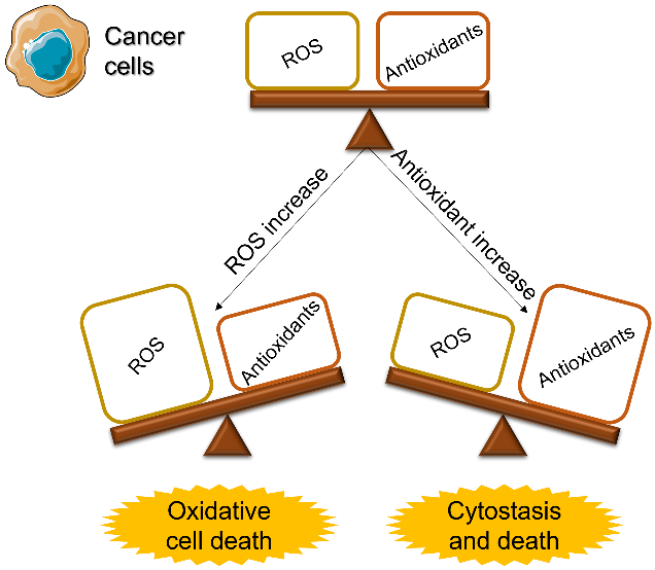

Figure 9 – Comparison of ROS and antioxidant levels and their consequences in cancer cells. Cancer cells normally contain higher levels of both ROS and antioxidants compared to healthy cells. If treatment with antioxidants is applied to these cells, the ROS levels will drop and cells will not be able to maintain their growth. If the ROS levels increase drastically, cells will suffer from oxidative stress and consequently death. Adapted from Sullivan, L. B. *et al.* [60]

Dietary supplements of antioxidants have been associated with cancer prevention for years. However, there are not consistent studies that prove the protective effects of antioxidants to scientifically support this association, being this a controversial topic[61]. Another debatable topic is antioxidant supplementation during chemotherapy, which is said to prevent and diminish the side effects. Antioxidants are expected to eliminate the excess of ROS that is produced by the tumor cells while they are suffering the effects of the anticancer agents, and that can affect the normal cells, but again, little scientific knowledge exists to support this theory[58]. In addition, recent research has appointed a direct anticancer effect to the antioxidants, attributing them the ability to induce cell death in tumor cells[61]. However, the results reported have not been consistent, for example, Sayin, V. I. *et al.* studied in 2014 the supplementation with N-acetylcysteine and vitamin E in mouse models of lung cancer and found that this supplementation increased tumor proliferation by reducing ROS production and p53 expression[62]. Nevertheless, some studies predict that this failure is due to the lack of specificity of these antioxidants[60].

As mitochondrial targeting has been one of the strategies to increase the specificity and reduce the toxicity of anticancer agents, researchers have been trying to develop drugs that can reduce the production of ROS in tumor cells by using mitochondria-targeted

antioxidants. The TPP cation can be a solution for the lack of specificity of antioxidants, as it can increase the mitochondrial concentration of the compound up to 1000 times, depending on the membrane potential[55]. A good example of this effect was performed by Cheng, G. *et al.* in 2013: they used a vitamin E analog conjugated with the TPP cation and found that it presented cytotoxic and anti-proliferative properties in breast cancer cell lines, and not in healthy cells[63].

Some compounds with antioxidant properties and containing the TPP moiety are also being used to try to protect the mitochondria and avoid its disruption as a therapeutic approach for pathologies such as Alzheimer's Disease[64]. In particular, a mitochondriotropic compound based on the natural antioxidant caffeic acid linked to the TPP moiety was developed by Teixeira, J. *et al.* in 2012[65] and was further improved, obtaining several derivatives in 2017[66]. One of these compounds contained a catechol group connected to the TPP moiety by a 10-carbon linker (Figure 10) and showed high toxicity and cell proliferation inhibition in human hepatocellular carcinoma HepG2 cells at concentrations as low as 2.5 μM[66]. The same compound, here called Mito6_TPP, was further studied by Benfeito, S. *et al.* in 2019, demonstrating a higher capacity to capture ROS than other compounds and showed cytotoxic properties in human neuroblastoma SH-SY5Y cells[67]. The authors predicted that the intrinsic lipophilicity related to the length of the alkyl linker might be one of the reasons that the cytotoxicity is observed on cells, together with the catechol group and/or the TPP moiety[67].

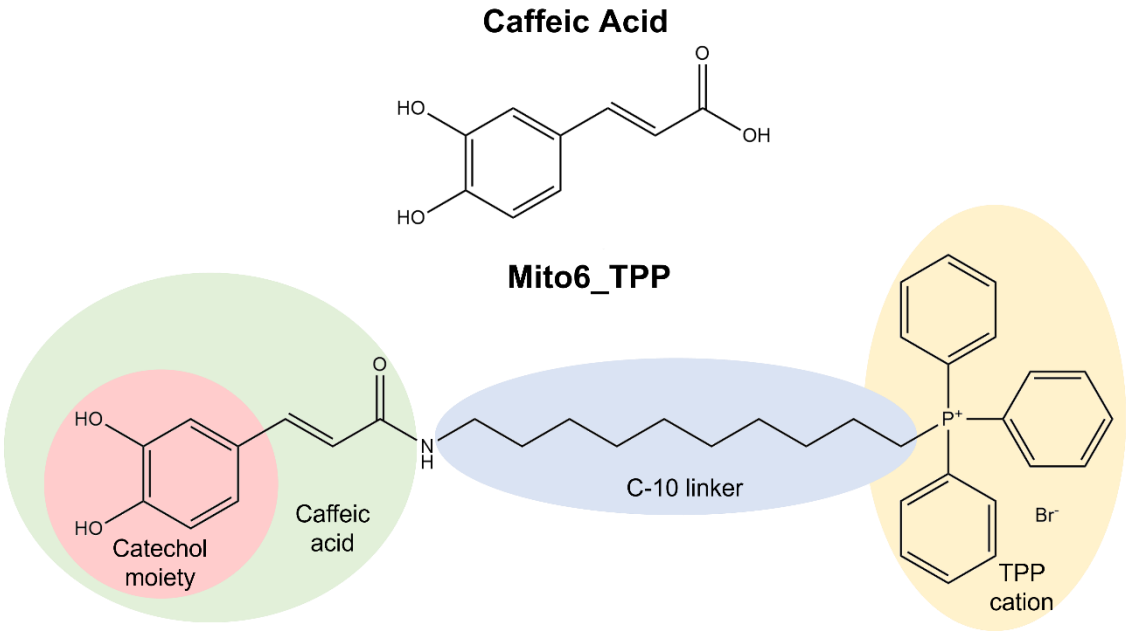

Figure 10 – Caffeic acid and its TPP-based derivative (Mito6_TPP) developed in the works of Teixeira, J. *et al.* and Benfeito, S. *et al.* Mito6_TPP is based on the caffeic acid and is constituted by a catechol moiety and a vinyl spacer connected to the TPP cation by a 10-carbon linker[66, 67].

The authors were looking for compounds able to prevent mitochondrial dysfunction and with neuroprotective properties against Alzheimer's disease. However, due to its cytotoxicity profile in HepG2 and SH-SY5Y cells this specific compound was not ideal to the main purpose, having the authors discarded it as a lead compound. Although the compound does not have applications for Alzheimer's disease as a mitochondria-targeted antioxidant, it might have other applications including against cancer. Moreover, the cell lines used in their studies were isolated from tumors and the compound showed cytotoxic effects against them, making it interesting to find out its anticancer potential.

6. Aim of the study

Ovarian and endometrial cancer are amongst the most frequent and most lethal cancers of the female reproductive system and, besides being related, their incidence is expected to increase. Treatment for both pathologies is mainly based on cytotoxic drugs, that bring unwanted side effects and are not specific. Interestingly, mitocans have been developed as promising anticancer agents, in particular, TPP-based compounds with antioxidant properties with good selectivity to induce cell death only in tumor cells.

As a result, this project aims to study the *in vitro* effects of the same TPP-based compound studied by Benfeito, S. *et al.*, here called Mito6_TPP, and two other compounds containing the same moieties, but with different cation carriers: one containing 4-picoline instead of TPP, here named Mito6_picol., and one containing isoquinoline instead of TPP, here called Mito6_isoq. (Figure 11).

The compounds were chosen due to the cytotoxic properties against tumor cells that each type of compound already demonstrated in other studies. These compounds will be tested in 4 cell lines: Ishikawa and Hec50co, two EC cell lines from type 1 and type 2, respectively, COV434, a GC tumor cell line, and HFF-1, an immortalized human foreskin fibroblasts cell line used as a control. The results of this study will evaluate the effectiveness of these compounds as possible anticancer agents against ovarian and endometrial cancer cells and their selectivity for tumor cells.

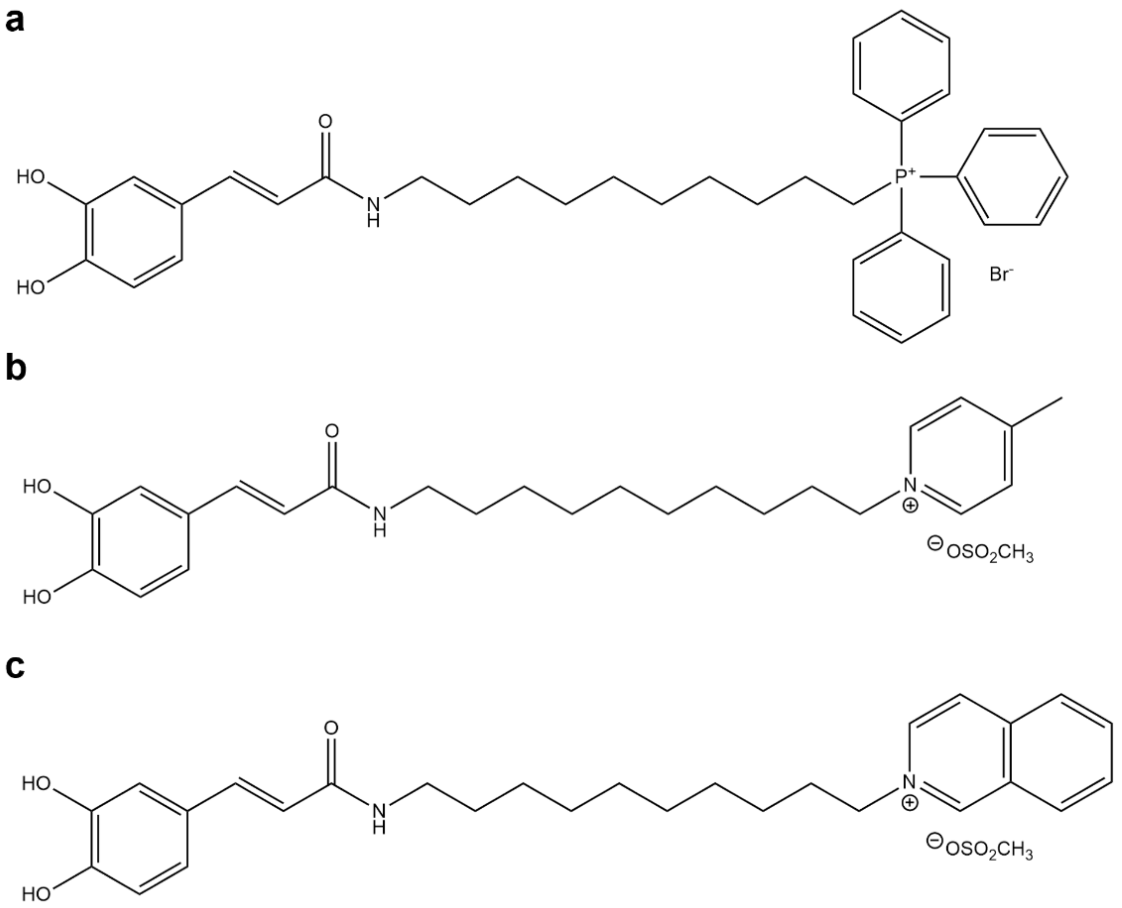

Figure 11 – Compounds used in this study. (a) Mito6_TPP: Molecular weight: 660,63, Chemical formula: $C_{37}H_{43}BrNO_3P$, IUPAC name: (E)-(10-(3-(3,4-dihydroxyphenyl)acrylamido)decyl)triphenylphosphonium bromide; **(b) Mito6_picol.:** Molecular weight: 506,66, Chemical formula: $C_{26}H_{38}N_2O_6S$, IUPAC name: (E)-1-(10-(3-(3,4-dihydroxyphenyl)acrylamido)decyl)-4-methylpyridin-1-ium methanesulfonate; **(c) Mito6_isoq.:** Molecular weight: 542,69, Chemical formula: $C_{29}H_{38}N_2O_6S$, IUPAC name: (E)-2-(10-(3-(3,4-dihydroxyphenyl)acrylamido)decyl)isoquinolin-2-ium methanesulfonate.

Materials and Methods

1. Materials

Dulbecco's Modified Eagle Medium/F12 (DMEM/F12), Roswell Park Memorial Institute 1640 (RPMI), methylthiazolyldiphenyl-tetrazolium bromide (MTT), hydrogen peroxide (H_2O_2), trypan blue Solution 0,4%, protease inhibitor cocktail (PI), Höechst 33342, carbonyl cyanide m-chlorophenylhydrazone (CCCP), 2,7- dichlorodihydrofluorescein diacetate (DCFH-DA), dimethyl sulfoxide (DMSO), Giemsa, sucrose and fluoroshield were from Sigma–Aldrich Co. St. Louis, MO, USA. All other reagents used were either from Sigma–Aldrich Co. St. Louis, MO, USA or Thermo Fisher, Life Technologies. Fetal bovine serum (FBS) was from Biochlome. Antibiotic-antimycotic (AB-AM) was from Grisp. Trypsin/EDTA 2,5% and 3,3′-dihexyloxacarbocyanine iodide ($DiOC_6$) was from Gibco/Invitrogen Corporation, Carlsbad, CA, USA. Pierce LDH cytotoxicity assay kit (LDH) was from Thermo Fisher, Life Technologies. Dibutylphthalate polystyrene xylene (DPX) was from VWR-Prolabo. Culture flasks were from Sarstedt and all the other plastic materials used in cell culture techniques were from Falcon TM, SD, USA or Nerbe plus.

2. Cell culture conditions

Experiments were performed using the following cell lines: Ishikawa, Hec50co, COV434, and HFF-1. Ishikawa cell line was established from an endometrial adenocarcinoma[28, 30]. Hec50co cell line consists of poorly differentiated endometrial tumor cells isolated from a patient with advanced disease[30]. COV434 is a human ovarian granulosa immortalized cell line established from a solid primary tumor[20]. And HFF-1 is an immortalized human foreskin fibroblasts cell line. Ishikawa and Hec50co cells were maintained in Dulbecco's Modified Eagle's Medium/F12 (DMEM/F12) supplemented with 5% of Foetal Bovine Serum (FBS). COV434 cells were maintained in DMEM/F12 10% FBS. And HFF-1 were maintained in Roswell Park Memorial Institute 1640 (RPMI 1640) supplemented with 10% FBS. All medium was supplemented with 1% of antibiotic-antimycotic (AB-AM) and all cells were kept at 37˚C with 5% CO_2. All cell lines were routinely harvested by trypsinization to new culture flasks when the confluence reached 70-80%. For the trypsinization, cells were washed with phosphate-buffered saline (PBS) and treated with 0.25% trypsin/EDTA for 4 minutes at 37°C. The collected cells were centrifuged at 400 *g* for 5 minutes at 4°C. The pellet containing the cells was resuspended in the respective cell culture medium. After that, live cells were counted using a hemocytometer and trypan blue. After counting the live cells, they were cultured in different flat-bottom plates: it was used the density of $5x10^4$ cells/well in transparent

and black 96-well plates. In 24-well plates, the densities were $1x10^5$ cells/well in Ishikawa and Hec50co and $2.5x10^5$ cells/well in COV434 and HFF. In 6-well plates, the density used was $8x10^5$ cells/well in COV434. The treatment with the compounds was done in the respective cell medium supplemented with 2% FBS, 24h after platting the cells in culture medium with 5% FBS, to allow their adherence.

3. Cell viability assays

3.1. MTT assay

Cell viability was evaluated using the tetrazolium salt [3-(4,5-dimetylthiazol-2-yl)-2,5-diphenyltetrazolium bromide] (MTT). This method is based on the fact that mitochondrial reductase enzymes are functional and metabolically active only in viable cells. These enzymes are capable of converting the yellow MTT salt into purple MTT formazan crystals, allowing to determine the cell viability spectrophotometrically (Figure 12)[68].

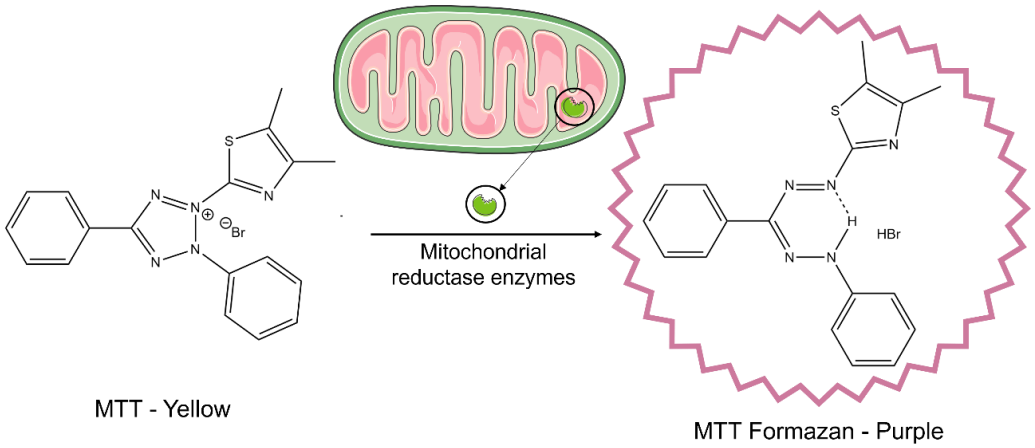

Figure 12 – Representation of the principle of the MTT assay. The yellow MTT salt is converted into the purple MTT formazan crystals by the mitochondrial reductase enzymes present in metabolic active and viable cells.

In order to carry out the MTT assay, all cell lines were plated, allowed to adhere for 24h and were then treated with medium supplemented with 2% FBS in the presence or absence of Mito6_TPP, Mito6_picol. or Mito6_isoq. (0.01 – 100 μM), in transparent 96-well plates and incubated at 37°C with 5% CO_2 for 24, 48 or 72 hours. Three wells containing only the highest concentration of the compound's vehicle (1% DMSO) were also added and showed no differences comparing to the control wells. The assay was performed based on the work by Moreira-Pinto, B. *et al.*[69]. After the incubation time, 5 mg/mL MTT was added to a final concentration of 0.5 mg/mL and cells were incubated for 3 hours at 37°C with 5% CO_2. After the 3 hours, purple MTT formazan crystals were formed, and the plate was agitated for 15 minutes to dissolve the crystals in a solution of DMSO/isopropanol (ratio 3:1). The quantity of MTT formazan crystals formed was quantified spectrophotometrically at 540 nm by using BioTek Synergy HTX Multi-Mode Microplate Reader equipped with BioTek Gen5 Data Collection and Analysis Software.

3.2. Neutral Red assay

Another assay used to determine cell viability was the Neutral Red (2-amino-3 methyl-7-dimethyl-aminophenazoniumchloride) assay. Neutral Red (NR) is a weakly cationic dye that can penetrate cell membranes and accumulate in the lysosomes of viable cells where it binds by hydrophobic bonds with anionic sites. While viable cells are able to incorporate the dye, non-viable cells are not[70]. Under acidic conditions, it is possible to revert this uptake and release the NR from the cells in order to quantify spectrophotometrically the amount of NR that was accumulated in the lysosomes. The quantity of NR released will be proportional to the quantity of viable cells (Figure 13).

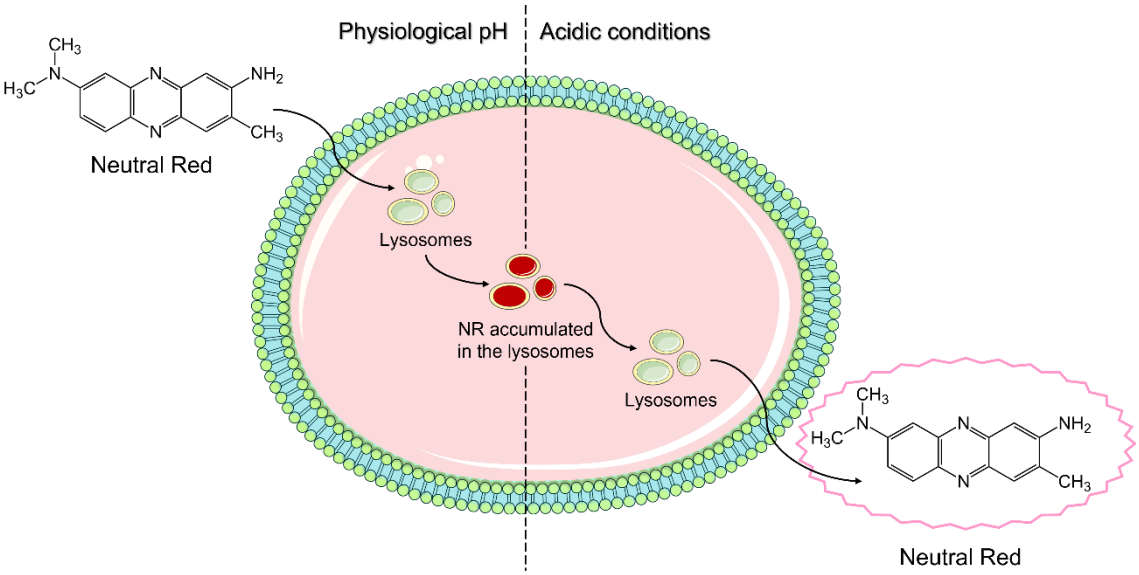

Figure 13 – Representation of the principle of the Neutral Red assay. The Neutral Red dye is able to cross the cell membrane at physiological pH, accumulating in the lysosomes of viable cells. After washing the cells, the dye will only be present in viable cells' lysosomes. In order to remove the NR to quantify it, it is necessary to submit these cells to acidic conditions.

To perform the NR assay, all cell lines were treated after adherence with medium 2% FBS in the presence or absence of Mito6_TPP, Mito6_picol. or Mito6_isoq. (0.01 – 100 μM) in transparent 96-well plates and incubated at 37°C with 5% CO_2 for 24, 48 or 72 hours. Three wells containing only the highest concentration of the compounds' vehicle (1% DMSO) were also added and showed no differences compared to the control wells. The assay was performed based on the work by Repetto G., *et al.*[71]. Briefly, after the incubation time, cells were washed with PBS and incubated with Neutral Red Medium (NRM) for 3 hours. NRM consists of a dilution of the Neutral Red Stock (4 mg/mL in PBS) in FBS-free cell medium at 40 μg/mL that was left at 37°C overnight and centrifuged at 900 *g* to remove precipitated dye crystals. After incubation time, cells were again washed with PBS, and incubated with Neutral Red Destain Solution (NRDS) at ambient temperature with shaking for 15 minutes. NRDS consists of a solution prepared with 50% ethanol (96% v/v), 49% deionized water and 1% glacial acetic acid. The NR extracted

from the cells was then measured at 540 nm by using BioTek Synergy HTX Multi-Mode Microplate Reader equipped with BioTek Gen5 Data Collection and Analysis Software.

4. Cytotoxicity assay – LDH assay

The activity of the enzyme lactate dehydrogenase (LDH) was measured to determine the cytotoxicity of the compounds in the cells. Since lactate dehydrogenase is a cytoplasmic oxidoreductase, when cells die by necrosis, this enzyme will be released into the culture medium. LDH in the cell culture medium will reduce NAD^+ to NADH through the oxidation of lactate to pyruvate. This assay evaluates the amount of LDH that was released through an enzymatic reaction that uses diaphorase to convert iodonitrotetrazolium (INT), a tetrazolium salt, into a red formazan product. The amount of color formed is proportional to the number of cells dying by necrosis (Figure 14)[72].

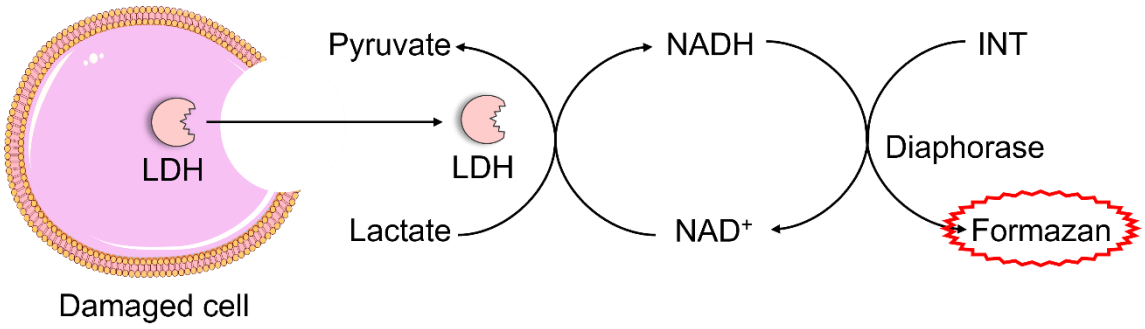

Figure 14 – Representation of the principle of the LDH assay. LDH catalyzes the oxidation of lactate to pyruvate through the reaction: NAD^+ to NADH. The diaphorase will then covert INT into the red formazan.

To start this experiment, Ishikawa, Hec50co and COV434 cells were treated after adherence with medium supplemented with 2% FBS in the presence or absence of Mito6_TPP, Mito6_picol. or Mito6_isoq. (1 – 20 μM) in transparent 96-well plates and incubated at 37°C with 5% CO_2 for 48 hours. Three wells containing only the highest concentration of the compounds' vehicle (1% DMSO) were also added and showed no differences compared to the control wells. The assay was not performed in HFF-1 cells due to the lack of evidence of cell death at the concentrations tested. After incubation time, the experiment was performed using Thermo Scientific Pierce LDH Cytotoxicity Assay Kit according to the manufacturer's instructions. Briefly, cell culture medium was incubated with Reaction Mix for 20 minutes in the dark. The reaction was then stopped using the Stop Solution. The intensity of red formazan was quantified at 490 nm using BioTek Synergy HTX Multi-Mode Microplate Reader equipped with BioTek Gen5 Data Collection and Analysis Software.

5. Mitochondrial membrane potential (Δψm) measurement

The dihexyloxacarbocyanine iodide ($DiOC_6$) probe was used to evaluate the Δψm. $DiOC_6$ is a green fluorescent lipophilic cationic dye, that is able to accumulate in the mitochondrial matrix in inverse proportion to the membrane potential. This means that a hyperpolarized mitochondria, where the interior is more negative, will accumulate more dye, and depolarized mitochondria accumulate less dye (Figure 15)[73].

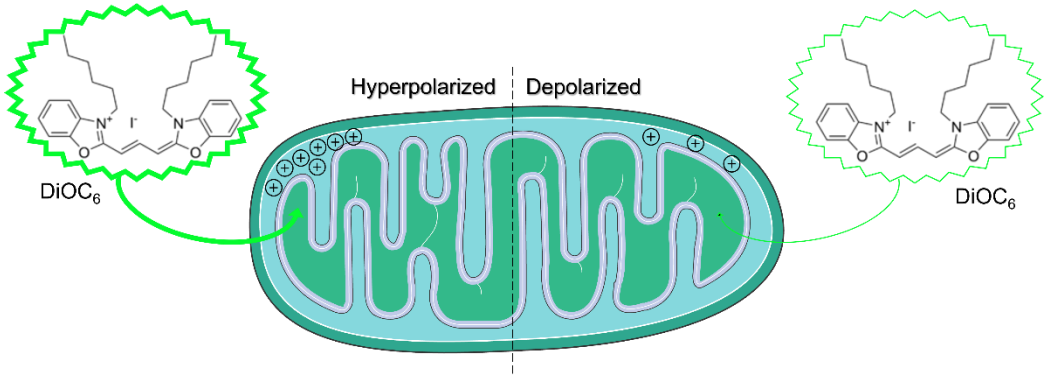

Figure 15 – Representation of the principle of the mitochondrial membrane potential (Δψm) measurement assay. $DiOC_6$ is a cationic green fluorescent dye that accumulates in the mitochondrial matrix depending on the membrane potential. A hyperpolarized mitochondria will be able to accumulate more dye than a depolarized mitochondria which has a less negative interior.

This experiment started by treating all cell lines after adherence with medium with 2% FBS in the presence or absence of 5 μM Mito6_TPP, 20 μM Mito6_picol. or 10 μM Mito6_isoq in black 96-well plates and incubated at 37°C with 5% CO_2 for 48 hours. The assay was conducted according to the work by Moreira-Pinto, B. *et al.*[69]. Three wells containing the mitochondrial membrane-depolarizing agent carbonyl cyanide m-chlorophenylhydrazone (CCCP) were also added as positive control at 50 μM for 20 minutes at 37°C with 5% CO_2 prior to the addition of the probe. All the wells were then washed with a solution of sucrose and protease inhibitor 0,05% in PBS (PBS/S/PI) and incubated with a 100 nM $DiOC_6$ solution for 30 minutes at 37 °C with 5% CO_2 in the dark. After the incubation period, the $DiOC_6$ solution was removed to eliminate the background fluorescence, new PBS/S/PI solution was added to the cells and the fluorescence was measured using BioTek Synergy HTX Multi-Mode Microplate Reader equipped with BioTek Gen5 Data Collection and Analysis Software (excitation: 485 nm; emission: 530 nm).

6. Cell morphology evaluation

The morphological changes in the cells after treatment with Mito6_TPP, Mito6_picol. or Mito6_isoq. were evaluated by phase-contrast microscopy and Giemsa and Höechst staining. The cells were cultured and treated without or with 5 μM Mito6_TPP, 20 μM Mito6_picol. or 10 μM Mito6_isoq. in 24-well plates with coverslips and incubated at 37°C

with 5% CO_2 for 72 hours. Cells evaluated by phase-contrast microscopy were observed using the Eclipse TS100 Inverted Microscope from Nikon equipped with an image analysis software NIKON NIS Elements.

6.1. Giemsa staining

Giemsa stain is a mixture of azure, methylene blue, and eosin dye, that is used as a differential staining to variably taint the various components of the cells. The eosin dye stains the basic components of the cells, while the methylene blue and the azure dyes stain the acidic components. The staining was performed according to the work by Moreira-Pinto, B. *et al.*[69]. After the end of the incubation time, culture medium was removed and all cell lines were washed with PBS, fixed with a solution of paraformaldehyde 4% in PBS for 15 minutes and stained with Giemsa solution diluted in distilled water (1:10) for 30 minutes. After that, the coverslips with stained cells were washed with tap water several times, dried and mounted in dibutylphthalate polystyrene xylene (DPX) medium. Cells were observed under microscope Eclipse CI, Nikon, Japan equipped with Nikon NIS Elements Image Software.

6.2. Höechst staining

Höechst is a dye that emits blue fluorescence when bound to DNA, it allows the evaluation of nuclear morphology and the identification of apoptotic cells by detecting the chromatin's condensation and fragmentation of the nuclei. The staining was performed based on the work by Crowley, L. C. *et al*.[74]. Briefly, Ishikawa, Hec50co and COV434 cells were first fixated with a solution of paraformaldehyde 4% in PBS for 15 minutes. The staining was not performed in HFF-1 cells due to the lack of evidence of cell death at the concentrations tested. The cells were then stained with 0.5 µg/mL Höechst in PBS for 20 minutes in the dark. After the staining time, cells were washed several times with PBS, mounted in Fluoroshield mounting medium and observed under a fluorescence microscope Eclipse CI, Nikon, Japan equipped with an excitation filter with maximum transmission at 360/400 nm and Nikon NIS Elements Image Software.

7. Intracellular reactive oxygen and nitrogen species (ROS/RNS) measurement

The 2',7'-dichlorodihydrofluorescein diacetate (DCFH-DA) probe was used to measure the levels of reactive oxygen/nitrogen species (ROS) generated after the treatment with the compounds. DCFH-DA is a lipophilic probe that can be taken up by cells and cleaved by esterases into 2',7'-dichlorodihydrofluorescein (DCFH), which is oxidized by ROS and forms the fluorescent molecule dichlorofluorescein (DCF) (Figure 16)[75].

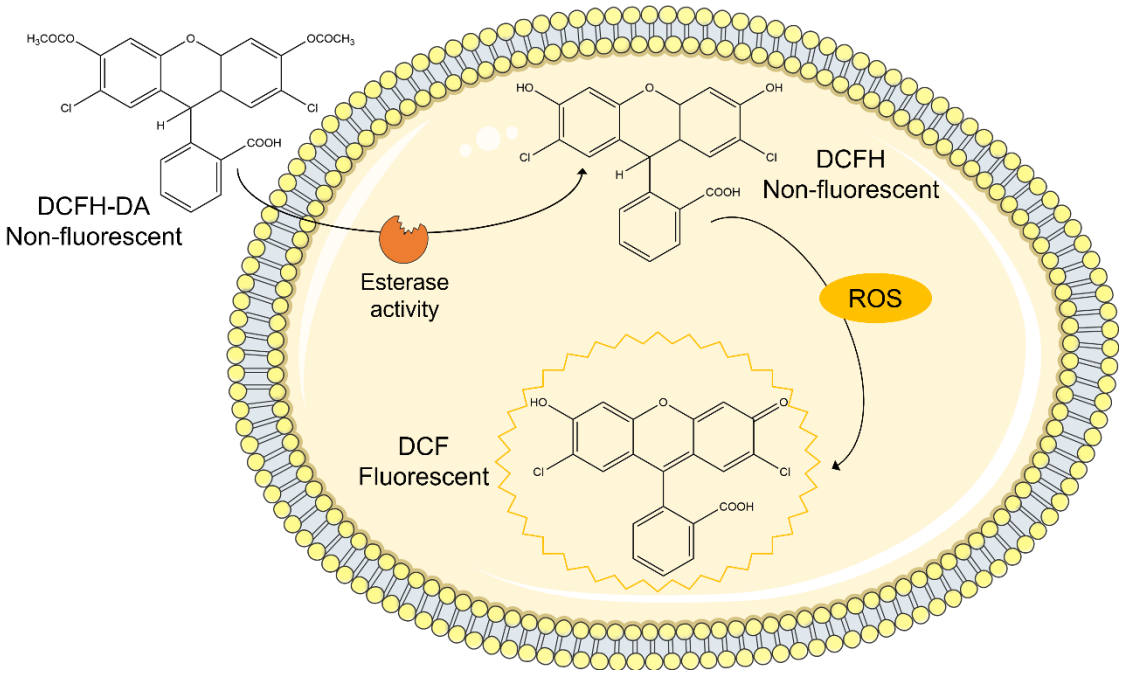

Figure 16 – Representation of the principle of the ROS measurement assay. Esterases inside the cells hydrolyze the DCFH-DA probe, forming DCFH which is oxidized by the free ROS to the fluorescent DCF.

This assay was performed immediately after the addition of the compounds. In order to do that, all cell lines were cultured in black 96-well plates and allowed to adhere for 24 hours at 37°C with 5% CO_2. This assay was conducted according to Bak, M.-J. *et al.*[76].After adherence of the cells, the culture medium was removed in all wells and cells were washed with PBS. Then, the cells were incubated with DCFH-DA at 25 μM for 1 hour at 37°C with 5% CO_2 in the dark. After the incubation period, cells were treated with culture medium with 2% FBS in the presence or absence of 5 μM Mito6_TPP, 20 μM Mito6_picol. or 10 μM Mito6_isoq. Three wells containing the stress inducer H_2O_2 were added as positive control at 200 μM. The fluorescence provided by DCF was measured immediately and every 5 minutes for 2 hours using BioTek Synergy HTX Multi-Mode Microplate Reader equipped with BioTek Gen5 Data Collection and Analysis Software (excitation: 485 nm; emission: 530 nm).

8. Western blot analysis

Western Blot is a technique that allows the detection of specific proteins contained in a mixture of other proteins. It permits the separation of all proteins by molecular weight and uses antibodies in order to visualize the protein of interest.

In this study, the protein of interest was PARP-1, as it is a substrate for several proteases participating in the apoptosis process, such as caspases, so the expression of a cleaved PARP-1 can be an indication of apoptosis. COV434 cells were cultured in transparent 6-well plates and treated after adherence with medium supplemented with 2% FBS in the

presence or absence of 5 μM Mito6_TPP, 20 μM Mito6_picol. or 10 μM Mito6_isoq. and incubated at 37°C with 5% CO_2 for 72 hours. After the incubation period, cells were reincubated with lysis buffer (20 mM Tris-HCl pH 7.5, 100 mM NaCl, 1 mM EDTA, 1% Triton X-100) containing 1% of protease inhibitors cocktail (PI) for 30 minutes on ice. Cells were then scrapped, collected, subjected to three cycles of freezing/thawing and centrifuged at 14 000 g for 10 minutes at 4 °C. The total protein concentration of each sample was determined through Bradford assay. All protein samples (25 μg) were prepared in sample buffer (1.56 M Tris pH 6.8, 1% SDS, 50% glycerol. 20% 2-mercaptoethanol, bromophenol blue 0.05%) and boiled for 5 minutes. The samples were then loaded in a 10% SDS–polyacrylamide gel and the electrophoresis started. At the end of the electrophoresis, the proteins were transferred onto nitrocellulose membranes using Trans-Blot Turbo (Trans-Blot®, Bio-Rad, USA) after a period of membrane activation of 10 minutes in transfer buffer (48 mM Tris-base, 39 mM Glycine, 20% methanol). The membranes were then incubated with blocking buffer (5% of dry milk in Tris-HCl Buffered Saline with 0.2% TWEEN 20® (TBS-TWEEN)) for 1 hour to block non-specific binding sites. After incubation time, membranes were left incubating overnight at 4°C with the primary antibody against mouse-cleaved PARP-1 (1:150; #sc-56196 Santa Cruz Biotechnology, CA, USA). Membranes were then washed with TBS-TWEEN and reincubated with secondary antibody anti-mouse (1:1000; Santa Cruz Biotechnology, CA, USA) for 2 hours, at room temperature. The membranes were then visualized using a chemiluminescence ChemiDocTMTouch Imaging System (Bio-Rad, Laboratories Melville, NY, USA) with Western Bright Detection Kit. The same membranes were also stripped by washing them with stripping solution (200 mM Glycine, 3.5 mM SDS, 1% TWEEN 20®, pH 2.2) twice for 5 minutes. After stripping, the membranes were washed with TBS and TBS-TWEEN and re-incubated with anti-β-actin antibody (1:500; Santa Cruz Biotechnology, CA, USA) for loading control.

9. Statistical analysis and software

The data was evaluated using the one- or two-way analysis of variance (ANOVA) test followed by Bonferroni's test for multiple comparisons. The data presented was expressed as mean±SEM (standard error of the mean) of at least three independent experiments performed in triplicate. Values of $p<0.05$ were considered statistically significant. The EC50 values were calculated by interpolation of dose-response curves and referred to as mean with 95% confidence interval (CI 95%). All statistical analysis was performed using GraphPad Prism software 8.0 (GraphPad PRISM v. 8.0, GraphPad Software, Inc., San Diego, CA, USA). Western blot analysis was carried in Image Lab software from Bio Rad. All images were created using Servier Medical Art.

Results

1. Ishikawa cell line

1.1. Cell viability and cytotoxicity

To investigate the effects of Mito6_TPP, Mito6_picol. and Mito6_isoq. on Ishikawa cell viability, the MTT and the Neutral red assays were performed. Cells were treated with the compounds in concentrations ranging from 0.01 μM to 100 μM and evaluated at 24, 48 or 72 hours of incubation.

As observed in Figure 17, Mito6_TPP induced a reduction in cell viability over 20 μM at 24h in both assays. At 48h, Mito6_TPP showed a reduction over 5 μM in the MTT assay and 10 μM in the NR assay. At 72h the decrease in cell viability caused by Mito6_TPP was significant over 1 μM in the MTT assay and 5 μM in the NR assay.

Mito6_picol. was the less effective compound: at 24h it had effects in concentrations over 20 μM using the MTT assay but had no significant effects using the NR assay. At 48h and 72h, Mito6_picol. caused a decrease over 20 μM using the MTT assay and over 50 μM in the NR assay (Figure 17).

It is visible in Figure 17 that Mito 6_isoq. induced decrease in cell viability at 24h over 20 μM only using the MTT assay and using the NR assay it was only statistically significant at 100 μM. At 48h and 72h, Mito6_isoq. caused a reduction in cell viability in concentrations over 10 μM using the MTT assay and over 50 μM in the NR assay.

Table 3 presents the EC50 of Mito6_TPP, Mito6_picol. and Mito6_isoq. in Ishikawa cells that were calculated in GraphPad Prism using the values obtained through the MTT assay and the NR assay that are included in the cell viability graphics from Figure 17. The results showed that the most effective compound, containing lower EC50 values, was the Mito6_TPP, followed by Mito6_isoq. and the least effective was the Mito6_picol. It is also visible that the effect of the compounds was time-dependent, meaning that the higher the time of incubation, the lower the EC50 was. They also showed that overall, the MTT assay allowed to obtain lower values of EC50 than the NR assay.

These inconsistencies in the EC50 obtained through MTT or NR assays might be explained by the different sensitivity of the techniques and the type of cells and type of compound tested[77]. This means that the values obtained will also vary more or less depending on the compound and cell line used, that is why it is recommended to perform more than one cell viability assay.

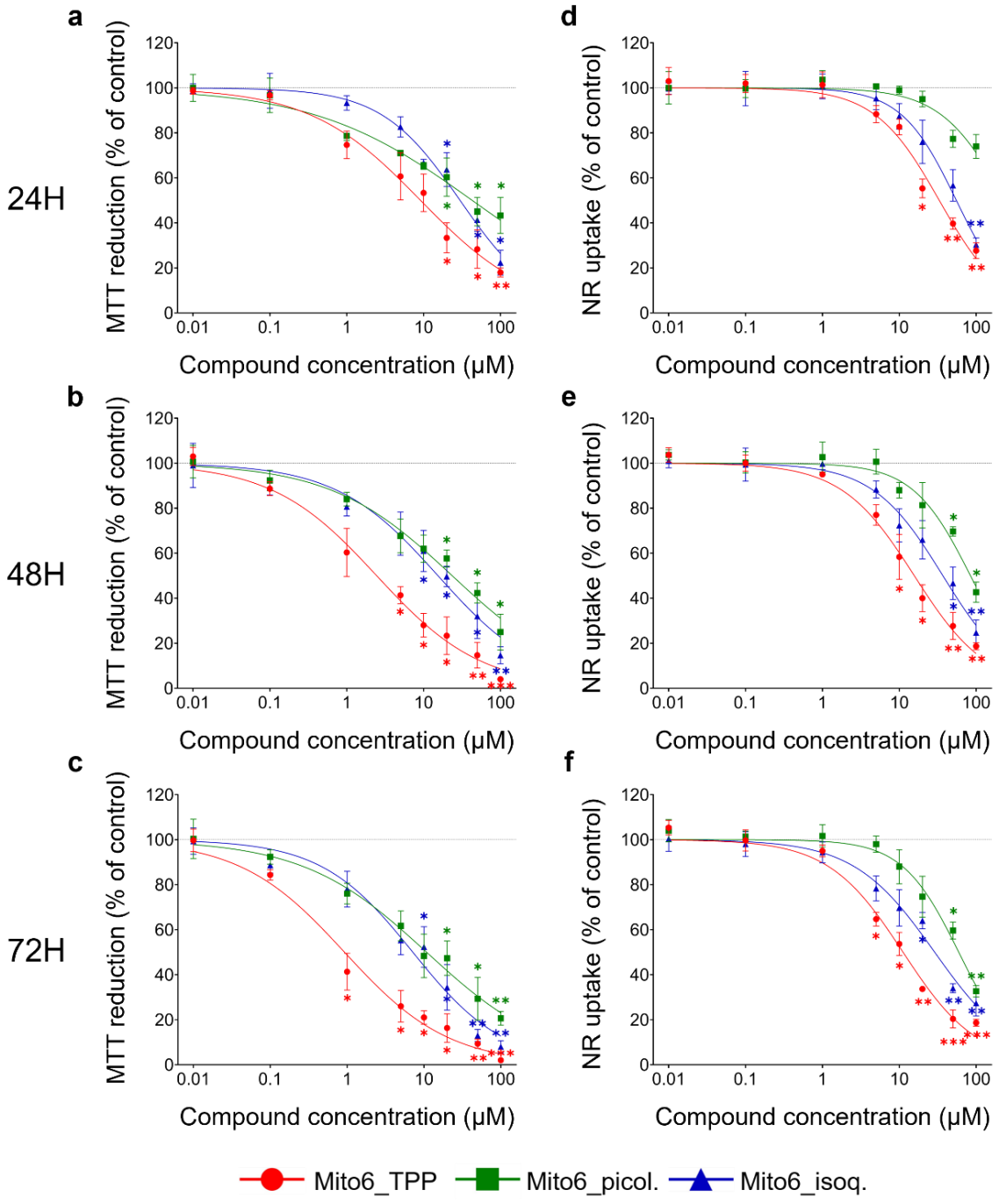

Figure 17 – Viability of Ishikawa cells treated with Mito6_TPP, Mito6_picol. or Mito6_isoq. (0,01-100 μM) at 24h, 48h and 72h of incubation. Viability assessed by MTT assay (a, b, c) and NR assay (d, e, f). Untreated cells were used as control. Control is represented as a dotted line at 100%. Results are compared to the control and expressed as mean ± SEM of at least three independent experiments performed in triplicate. Significant differences between treated and untreated cells are described as * ($p<0,05$), ** ($p<0,01$) and *** ($p<0,001$).

Table 3 – EC50 of Mito6_TPP, Mito6_picol. and Mito6_isoq. in Ishikawa cells at 24h, 48h, 72h of incubation. The values were calculated by GraphPad Prism using the decrease of viability obtained through the MTT or the NR assay. [1]CI: Confidence Interval at 95%.

	EC50 (μM) – Mean (CI 95%)[1]					
	MTT assay			NR assay		
	Mito6_TPP	Mito6_picol.	Mito6_isoq.	Mito6_TPP	Mito6_picol.	Mito6_isoq.
24h	9.142 (7.047 - 11.73)	42.92 (31.09 - 63.27)	29.85 (25.36 - 3535)	33.16 (28.58 - 38.72)	>100 ---	55.29 (48.02 - 64.32)
48h	2.453 (1.859 - 3.188)	23.56 (18.36 - 30.69)	15.39 (11.49 - 20.39)	15.69 (13.47 - 18.29)	84.44 (70.97 - 105.2)	36.94 (31.15 - 44.21)
72h	0.9248 (0.6905 - 1.225)	10.80 (8.142 - 14.23)	7.160 (5.313 - 9.380)	11.19 (9.659 - 12.94)	59.40 (51.37 - 69.61)	28.88 (24.37 - 34.48)

The cytotoxicity of Mito6_TPP, Mito6_picol. and Mito6_isoq. on Ishikawa cells was evaluated through the LDH release assay. Cells were treated with the compounds in the lower concentrations that induced decrease in cell viability (1-20 μM) and were evaluated at 48 hours of incubation. In the concentrations tested, only Mito6_TPP at 20 μM of showed to be cytotoxic to Ishikawa cells, increasing the LDH release by 31% (Figure 18).

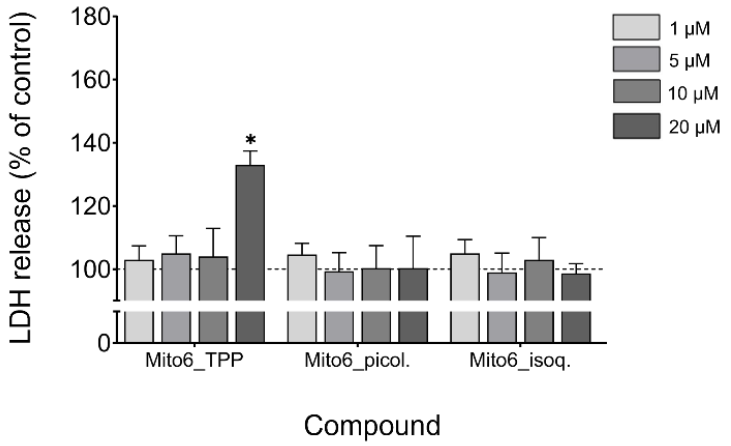

Figure 18 – Cytotoxicity of Mito6_TPP, Mito6_picol. or Mito6_isoq. (1-20 μM) in Ishikawa cells after 48h of incubation. Cytotoxicity assessed by LDH release assay. Untreated cells were used as control. Control is represented as a dotted line at 100%. Results are compared to the control and expressed as mean ± SEM of at least three independent experiments performed in triplicate. Significant differences between treated and untreated cells are described as * (p<0,05).

1.2. Mitochondrial membrane potential (Δψm)

The influence of Mito6_TPP, Mito6_picol. and Mito6_isoq. on Ishikawa cells' Δψm was assessed using a fluorescence assay with $DiOC_6$ probe. Cells were treated with 5 μM of Mito6_TPP, 20 μM of Mito6_picol. and 10 μM of Mito6_isoq. and left incubation for 48 hours. The concentrations were chosen due to the data regarding cell viability and cytotoxicity in all cell lines, as they induced decrease in cell viability in all tumor cell lines, but did not prove to be cytotoxic in any of them.

Results showed that all compounds induced a decrease in Δψm in the tested concentrations, being Mito6_TPP the most potent, as it induced a decrease of 55% in Δψm with only 5 μM of compound (Figure 19).

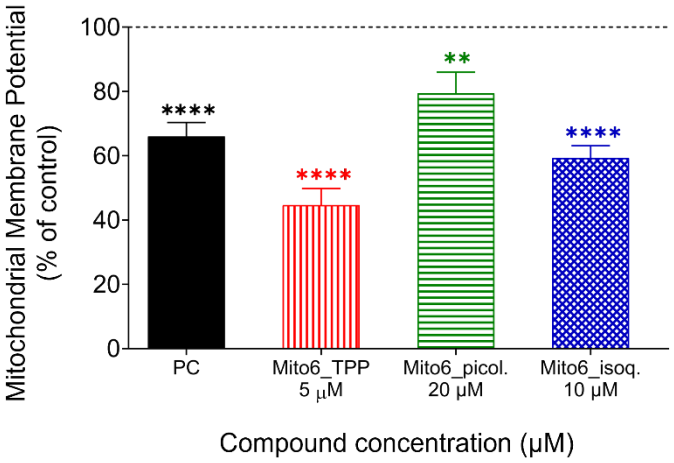

Figure 19 – Mitochondrial membrane potential of Ishikawa cells after 48h of incubation with 5 μM of Mito6_TPP, 20 μM of Mito6_picol. or 10 μM of Mito6_isoq. Δψm assessed by fluorescence assay with $DiOC_6$ probe. Untreated cells were used as control. CCCP (50 μM) was used as positive control (PC). Control is represented as a dotted line at 100%. Results are compared to the control and expressed as mean ± SEM of at least three independent experiments performed in triplicate. Significant differences between treated and untreated cells are described as *** (p<0,001) and **** (p<0,0001).

1.3. Cell morphology

Morphological changes in Ishikawa cells induced by the compounds were directly observed under a phase contrast microscope or first stained with either Giemsa or Höechst. Cells were treated with the tested concentration of each compound: 5 μM of Mito6_TPP, 20 μM of Mito6_picol. and 10 μM of Mito6_isoq. and observed at 72 hours of incubation. The concentrations were chosen based on the data about cell viability and cytotoxicity, as these concentrations provoked a decrease in cell viability in all tumor cell lines, but were not cytotoxic in any of them, allowing the observation of cell morphology.

The images shown in Figure 20 were considered to be representative of all assays. Mito6_TPP was the compound that induced more morphological changes in this cell line: in the phase contrast microscopy and Giemsa staining, it was possible to notice a clear reduction in cell density, as well as an altered shape of the whole cell and its nucleus. In Giemsa staining, as well as in Höechst staining there were some signs of chromatin condensation, and in Höechst staining, there was also visible some nucleus fragmentation.

Mito6_picol. was the least effective compound as it did not induce morphological changes: it was only possible to visualize a small reduction in cell density in phase contrast microscopy and Giemsa staining. Other changes such as cell deformation or chromatin condensation were not visible (Figure 20).

Mito6_isoq. had more effects than Mito6_picol. but fewer effects than Mito6_TPP: in the phase contrast microscopy and Giemsa staining, it was visible a small reduction in cell density and an altered shape of the whole cell. In Giemsa staining and Höechst staining, there were some signs of chromatin condensation, although no nucleus fragmentation was present (Figure 20).

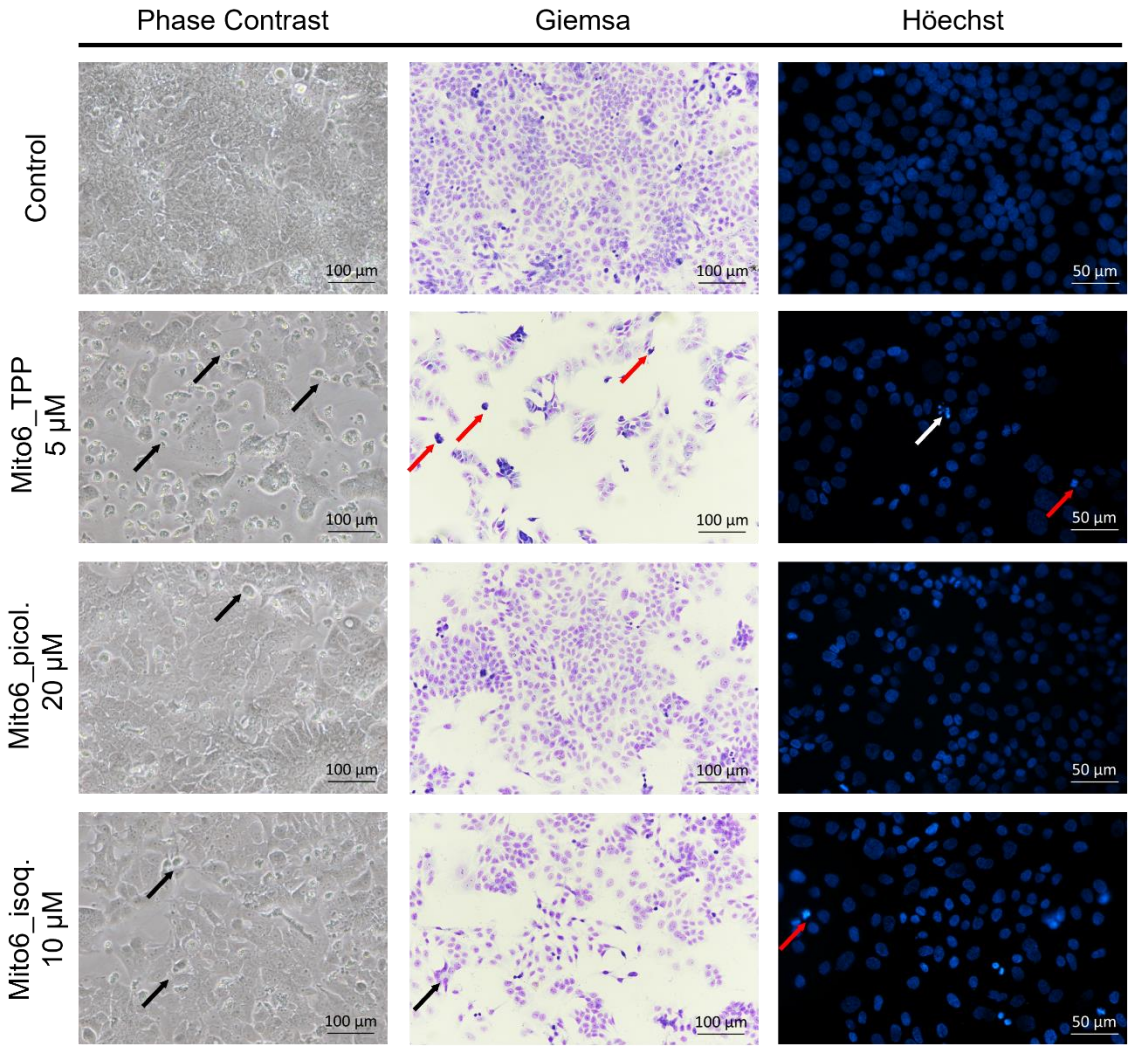

Figure 20 – Morphology of Ishikawa cells after 72h of incubation with 5 µM of Mito6_TPP, 20 µM of Mito6_picol. or 10 µM of Mito6_isoq. Morphology assessed by phase contrast, Giemsa and Höechst staining. Untreated cells were used as control. Black arrows indicate abnormal cell morphology; Red arrows indicate chromatin condensation; White arrows indicate nucleus fragmentation.

1.4. Intracellular reactive oxygen and nitrogen species (ROS/RNS) levels

A fluorescence assay with DCFH-DA was performed to evaluate the consequences of Mito6_TPP, Mito6_picol. and Mito6_isoq. on Ishikawa cells' ROS levels. Cells were incubated with the DCFH-DA probe for 1 hour, and 10 µM of each compound were added at the end of the incubation. This concentration was chosen as it was the intermediate concentration between the ones used for the Δψm measurement and analysis of cell morphology. ROS levels were measured for 2 hours immediately after treatment.

The results showed a significant decrease in ROS release after incubation with all the compounds. However, Mito6_TPP was the most potent compound, inducing a significant decrease starting at only 10 minutes of incubation and reaching a 60% reduction at the end of the 2h. The other two compounds only started to have significant decreases at 25 and 35 minutes, and decreased only to a maximum of 79% or 70% of the initial concentration for Mito6_picol. and Mito6_isoq., respectively (Figure 21).

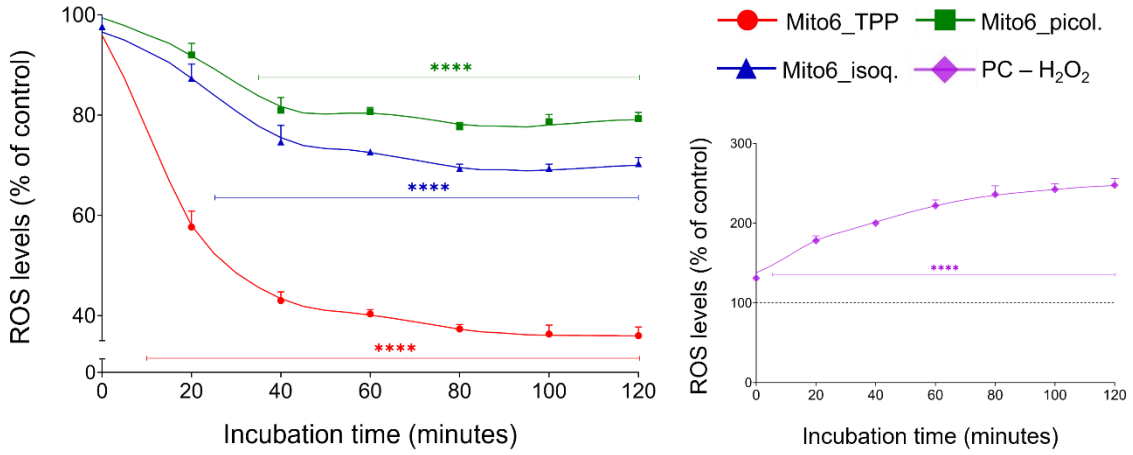

Figure 21 – Intracellular ROS levels in Ishikawa cells in the 2h immediately after the addition of 10 μM of Mito6_TPP, Mito6_picol. or Mito6_isoq. Left: ROS release assessed by fluorescence assay with DCFH-DA probe. Untreated cells were used as control. **Right:** H_2O_2 (200 μM) was used as positive control. Control is represented as a dotted line at 100%. Results are compared to the control and expressed as mean of at least three independent experiments performed in triplicate. Significant differences between treated and untreated cells are described as **** (p<0,0001).

2. Hec50co cell line

2.1. Cell viability and cytotoxicity

The effects of Mito6_TPP, Mito6_picol. and Mito6_isoq. on Hec50co cell viability, were evaluated through the MTT and the Neutral red assays. Cells were incubated with the compounds in different concentrations (0.01-100 μM) and the assays were performed at 24, 48 or 72 hours of incubation.

As observed in Figure 22, Mito6_TPP was the most potent compound: at 24h of incubation it induced reduction in cell viability in concentrations over 5 μM using the MTT assay and over 50 μM using the NR assay. At 48h and 72h, the decrease in cell viability started at 5 μM in the MTT assay and 20 μM in the NR assay.

Mito6_picol was the least effective: at 24h induced reduction in cell viability over 50 μM and showed no effects in NR assay, at 48h the effects were significant over 20 μM using MTT assay but were not significant using NR assay and at 72h were significant over 10 μM in the MTT assay and at 100 μM in the NR assay (Figure 22).

Mito6_isoq. induced cell viability decrease at 24h in concentrations over 10 μM in the MTT assay, and at 48h and 72h, it induced reduction over 5 μM. Using the NR in any incubation time it was necessary to have 100 μM to induce reduction of cell viability.

Table 4 presents the EC50 of Mito6_TPP, Mito6_picol. and Mito6_isoq. in Hec50co cells that were calculated with the values of cell viability that are included in Figure 22. The most effective compound was Mito6_TPP, which presented lower EC50 values, followed by Mito6_isoq. and Mito6_picol. Once again, the effect of the compounds was time-dependent and presented lower EC50 with higher times of incubation. In addition, the MTT assay presented lower values of EC50 than the NR assay.

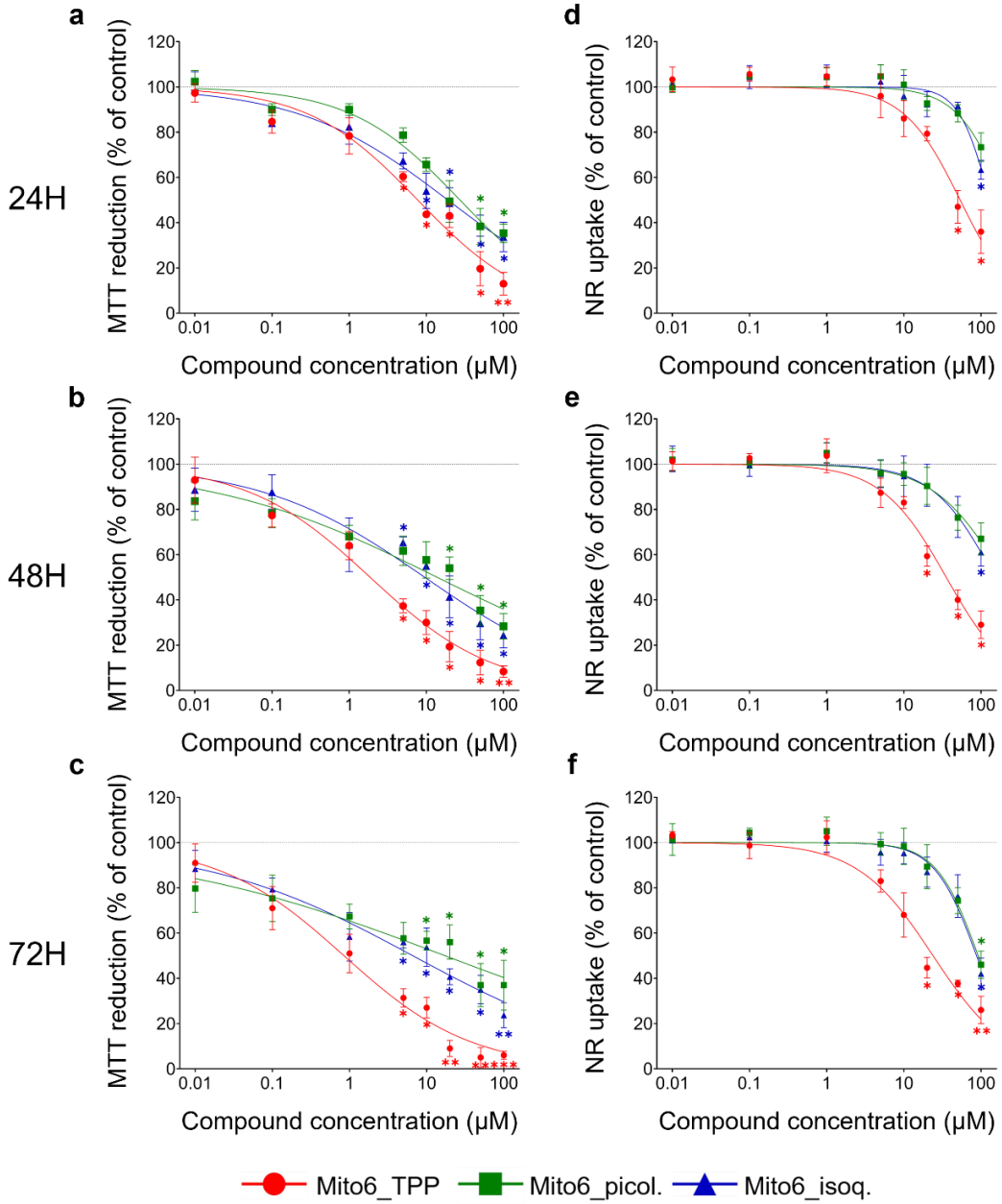

Figure 22 – Viability of Hec50co cells treated with Mito6_TPP, Mito6_picol. or Mito6_isoq. (0,01-100 μM) at 24h, 48h and 72h of incubation. Viability assessed by MTT assay (a, b, c) and NR assay (d, e, f). Untreated cells were used as control. Control is represented as a dotted line at 100%. Results are compared to the control and expressed as mean ± SEM of at least three independent experiments performed in triplicate. Significant differences between treated and untreated cells are described as * (p<0,05), ** (p<0,01) and *** (p<0,001).

Table 4 – EC50 of Mito6_TPP, Mito6_picol. and Mito6_isoq. in Hec50co cells at 24h, 48h, 72h of incubation. The values were calculated by GraphPad Prism using the decrease of viability obtained through the MTT or the NR assay. [1]CI: Confidence Interval at 95%.

	EC50 (μM) – Mean (CI 95%)[1]					
	MTT assay			NR assay		
	Mito6_TPP	Mito6_picol.	Mito6_isoq.	Mito6_TPP	Mito6_picol.	Mito6_isoq.
24h	7.746 (5.836 - 10.07)	27.33 (21.57 - 35.43)	19.02 (14.08 - 26.23)	53.65 (44.62 - 65.82)	>100 ---	>100 ---
48h	1.872 (1.355 - 2.530)	13.82 (8.240 - 24.37)	9.554 (6.105 - 14.78)	35.41 (30.32 - 41.67)	>100 ---	>100 ---
72h	0.8468 (0.5669 - 1.235)	17.24 (8.418 - 42.24)	6.590 (4.170 - 10.35)	23.87 (19.35 - 29.75)	92.01 (79.42 - 111.8)	87.58 (76.49 - 104.7)

To evaluate the cytotoxicity of the compounds on Hec50co cells, the LDH release assay was performed. Cells were treated with the compounds in the lower concentrations that induced cell viability reduction (1-20 μM) and the experiment was performed at 48 hours of incubation. The results showed that no concentration of any compound induced a significant increase in LDH release in Hec50co cells. Although it is not statistically significant, 20 μM of Mito6_TPP already showed a tendency to be cytotoxic to Hec50co cells (Figure 23).

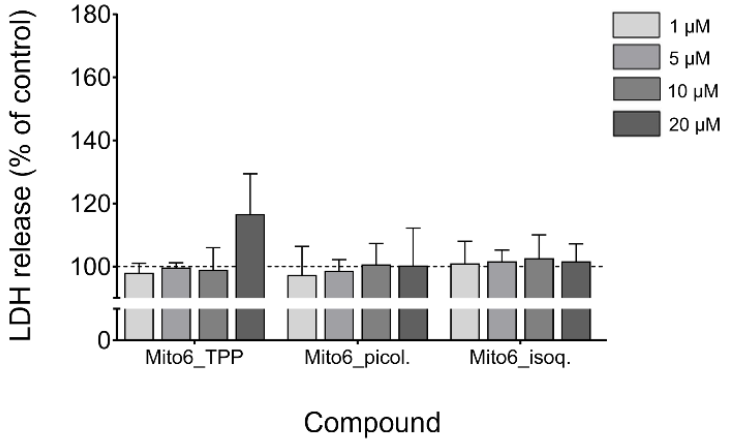

Figure 23 – Cytotoxicity of Mito6_TPP, Mito6_picol. or Mito6_isoq. (1-20 μM) in Hec50co cells after 48h of incubation. Cytotoxicity assessed by LDH release assay. Untreated cells were used as control. Control is represented as a dotted line at 100%. Results are compared to the control and expressed as mean ± SEM of at least three independent experiments performed in triplicate. No significant differences between treated and untreated cells were detected.

2.2. Mitochondrial membrane potential (Δψm)

The impact of Mito6_TPP, Mito6_picol. and Mito6_isoq. on the Δψm of Hec50co cells, was assessed using a fluorescence assay with $DiOC_6$ probe. Cells were incubated with one concentration of each compound: 5 μM of Mito6_TPP, 20 μM of Mito6_picol. and 10 μM of Mito6_isoq. and the experiment was performed at 48 hours of incubation. The criteria to choose these concentrations was the same applied to Ishikawa cells.

Results showed that only Mito6_TPP and Mito6_isoq. were able to induce a significant reduction on the Δψm. Once again, Mito6_TPP at 5 μM was the most potent compound, reducing the Δψm to 74% comparing to the control cells (Figure 24).

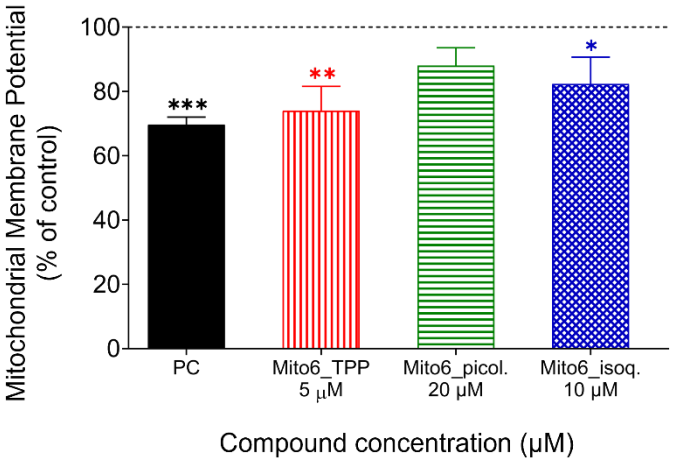

Figure 24 – Mitochondrial membrane potential of Hec50co cells after 48h of incubation with 5 μM of Mito6_TPP, 20 μM of Mito6_picol. or 10 μM of Mito6_isoq. Δψm assessed by fluorescence assay with $DiOC_6$ probe. Untreated cells were used as control. CCCP (50 μM) was used as positive control (PC). Control is represented as a dotted line at 100%. Results are compared to the control and expressed as mean ± SEM of at least three independent experiments performed in triplicate. Significant differences between treated and untreated cells are described as * (p<0,05), ** (p<0,01) and *** (p<0,001).

2.3. Cell morphology

Changes in the morphology of Hec50co cells induced by Mito6_TPP, Mito6_picol. or Mito6_isoq. were observed directly under a phase contrast microscope or observed stained with either Giemsa or Höechst. Cells were treated with one concentration of each compound: 5 μM of Mito6_TPP, 20 μM of Mito6_picol. and 10 μM of Mito6_isoq. and photographed at 72 hours of incubation. The criteria to choose these concentrations was the same applied to Ishikawa cells.

The images shown in Figure 25 were considered to be representative of all assays. Results showed that Mito6_TPP was the most effective compound inducing more morphological changes than the other two compounds: in the phase contrast microscopy and Giemsa staining, it was visible a drastic cell density decrease and an altered shape of the cell and its nucleus. In Giemsa staining, as well as in Höechst staining there were some signs of chromatin condensation.

Mito6_picol. was the least effective compound showing no effect in cell morphology (Figure 25).

Mito6_isoq. induced only a few morphological changes: in the phase contrast microscopy and Giemsa staining, it was visible a small reduction in cell density. Only an altered shape of the nucleus was clear in Höechst staining (Figure 25).

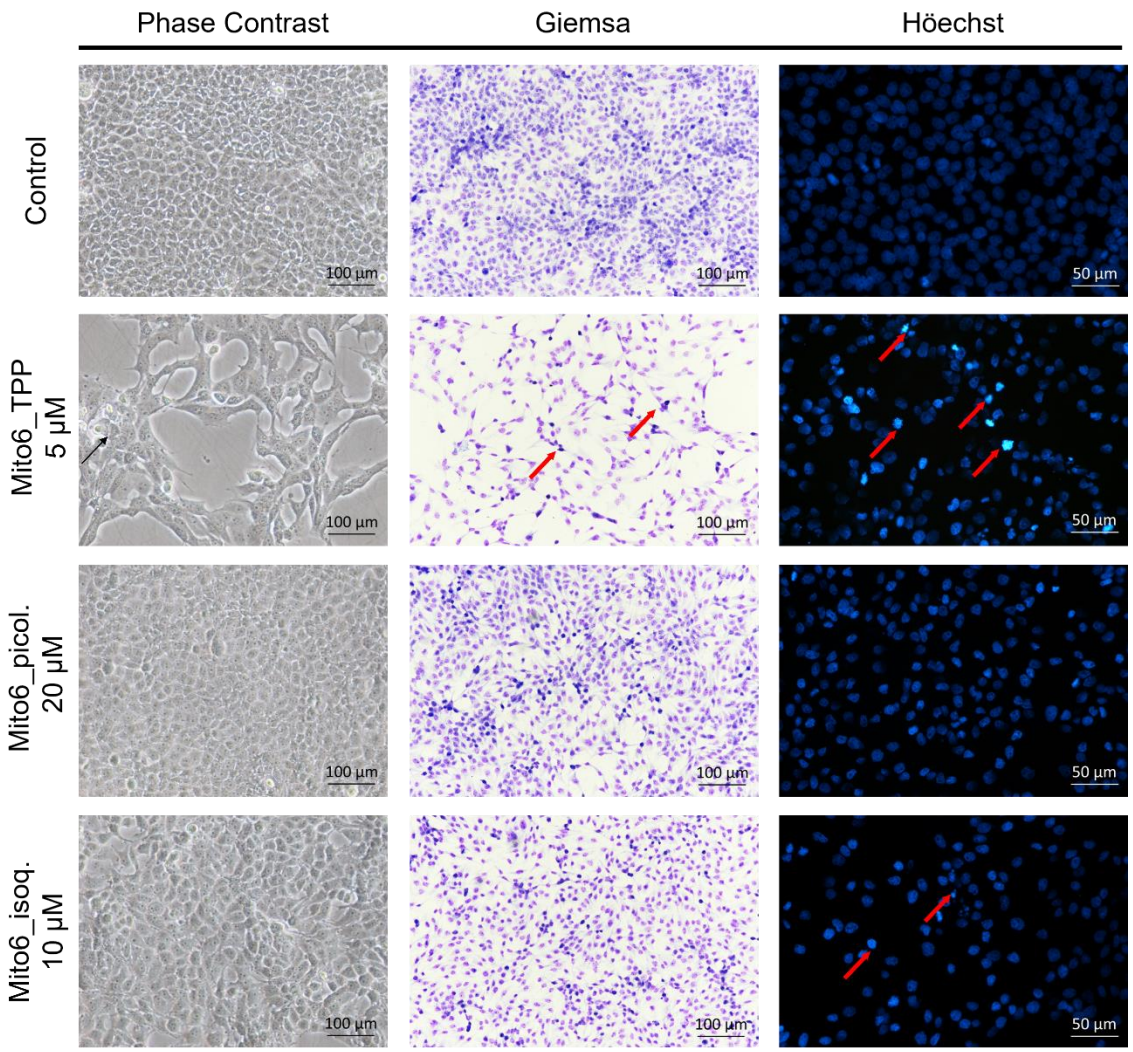

Figure 25 – Morphology of Hec50co cells after 72h of incubation with 5 µM of Mito6_TPP, 20 µM of Mito6_picol. or 10 µM of Mito6_isoq. Morphology assessed by phase contrast, Giemsa and Höechst staining. Untreated cells were used as control. Black arrows indicate abnormal cell morphology; Red arrows indicate chromatin condensation.

2.4. Intracellular reactive oxygen and nitrogen species (ROS/RNS) levels

To evaluate the effects of Mito6_TPP, Mito6_picol. and Mito6_isoq. on Hec50co cells' ROS levels, a fluorescence assay with DCFH-DA was performed. Cells were treated with 10 µM of each compound after incubation with the DCFH-DA probe. This concentration was chosen for the same reason as in Ishikawa cells. ROS release was then measured for 2 hours immediately after treatment.

All compounds were able to induce a significant decrease in ROS release, but Mito6_TPP showed to be the compound with a more drastic reduction. Mito6_TPP had effects starting at 15 minutes and reached 55% of the control at the end of the 2h of incubation. Mito6_isoq. showed effects at 25 minutes and reached 82% of the control. And Mito6_picol. had effects at 35 minutes of incubation and reached only 85% of the control (Figure 26).

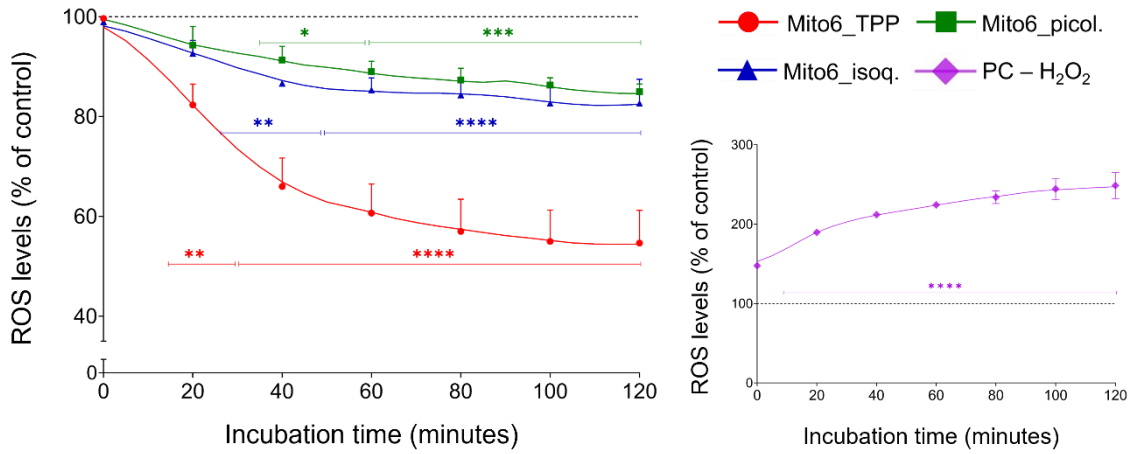

Figure 26 – Intracellular ROS levels by Hec50co cells in the 2h immediately after the addition of 10 µM of Mito6_TPP, Mito6_picol. or Mito6_isoq. Left: ROS release assessed by fluorescence assay with DCFH-DA probe. Untreated cells were used as control. **Right:** H_2O_2 (200 µM) was used as positive control. Control is represented as a dotted line at 100%. Results are compared to the control and expressed as mean of at least three independent experiments performed in triplicate. Significant differences between treated and untreated cells are described as * (p<0,05), ** (p<0,01), *** (p<0,001) and **** (p<0,0001).

3. COV434 cell line

3.1. Cell viability and cytotoxicity

The effects of Mito6_TPP, Mito6_picol. and Mito6_isoq. on COV434 cell viability, were evaluated using the MTT and the Neutral red assays. Cells were treated with the compounds in concentrations varying from 0.01 µM to 100 µM and the experiment was conducted at 24, 48 or 72 hours of incubation.

As observed in Figure 27, Mito6_TPP was the most potent compound: it induced a reduction in cell viability over 1 µM at 24h using the MTT assay and 10 µM using the NR assay. At 48h showed effects over 1 µM in the MTT assay and 5 µM in the NR assay. At 72h the reduction in cell viability was visible over 1 µM in the MTT assay and 5 µM in the NR assay.

Mito6_picol. was the less potent of all compounds: at 24h it showed to decrease cell viability in concentrations over 5 µM using the MTT assay and had no significant effects using the NR assay. At 48h the effects started at 5 µM using the MTT assay and at 50 µM in the NR assay. And at 72h the decrease started over 1 µM using the MTT assay and over 50 µM in the NR assay (Figure 27).

Mito 6_isoq. was the second most potent compound: at 24h the reduction in cell viability was significant over 5 µM using the MTT assay and using the NR assay it was significant at 50 µM, and at 48h and 72h the decrease in cell viability was significant in concentrations over 1 µM using the MTT assay and over 50 µM in the NR assay (Figure 27).

The EC50 of all compounds in COV434 cells is present in Table 5 and was calculated using GraphPad Prism and the values obtained through the MTT assay and the NR included in the graphics from Figure 27. The most effective compound was Mito6_TPP, Mito6_isoq. was the second most potent and the least effective compound was Mito6_picol. It is also possible to conclude that the effect of the compounds was time-dependent and the higher the time of incubation, the lower the EC50 was. Results showed that in this case, the MTT assay resulted in lower values of EC50 than the NR assay.

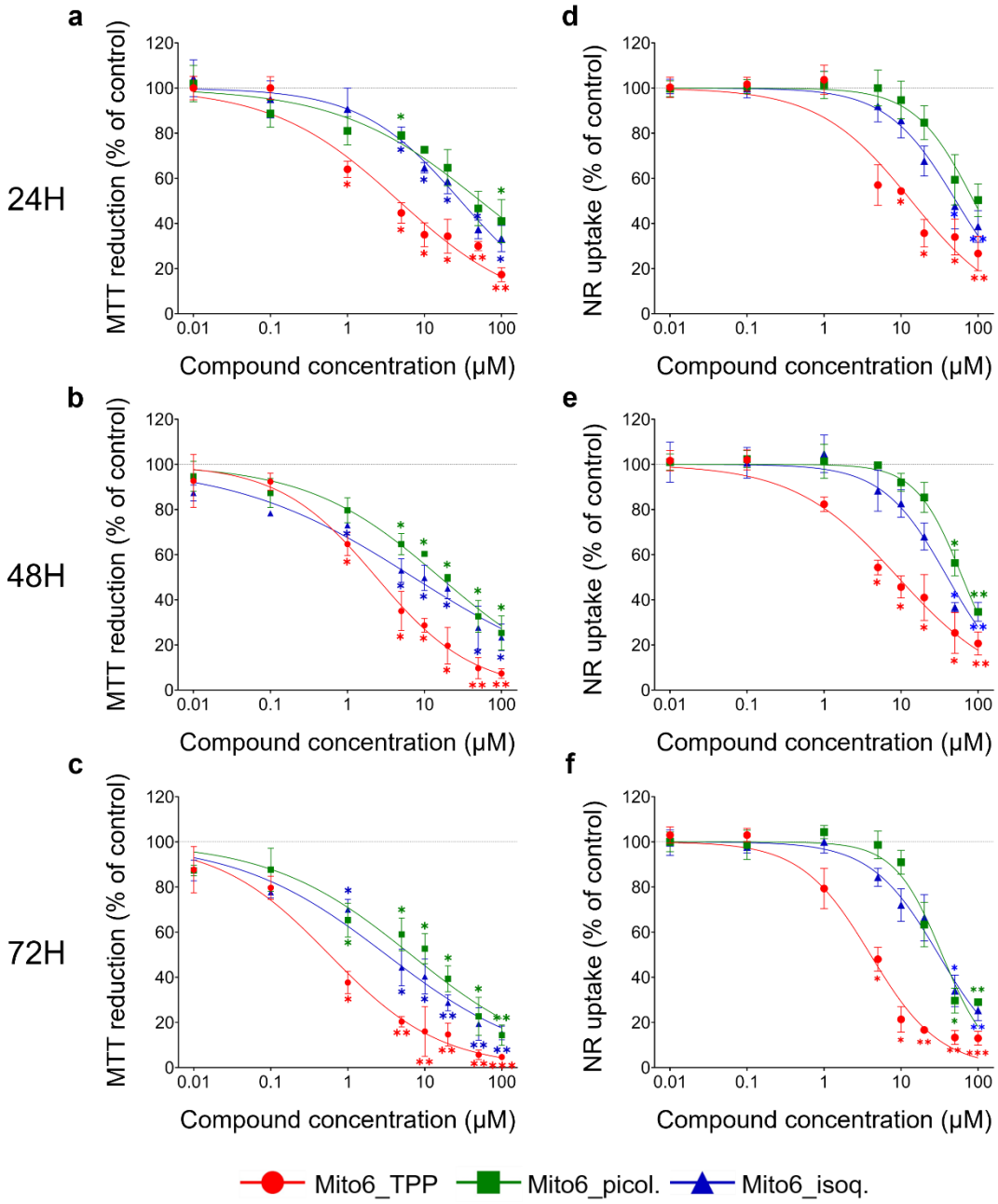

Figure 27 – Viability of COV434 cells treated with Mito6_TPP, Mito6_picol. or Mito6_isoq. (0,01-100 μM) at 24h, 48h and 72h of incubation. Viability assessed by MTT assay (a, b, c) and NR assay (d, e, f). Untreated cells were used as control. Results are compared to the control and expressed as mean ± SEM of at least three independent experiments performed in triplicate. Significant differences between treated and untreated cells are described as * (p<0,05), ** (p<0,01) and *** (p<0,001).

Table 5 – EC50 of Mito6_TPP, Mito6_picol. and Mito6_isoq. in COV434 cells at 24h, 48h, 72h of incubation. The values were calculated by GraphPad Prism using the decrease of viability obtained through the MTT or the NR assay. [1]CI: Confidence Interval at 95%.

	EC50 (μM) – Mean (CI 95%)[1]					
	MTT assay			NR assay		
	Mito6_TPP	Mito6_picol.	Mito6_isoq.	Mito6_TPP	Mito6_picol.	Mito6_isoq.
24h	4.644 (3.317 - 6.418)	53.21 (36.54 - 88.56)	29.5 (23.61 - 37.58)	13.62 (9.671 - 19.38)	87.76 (70.73 - 117.0)	51.62 (42.41 - 64.49)
48h	2.367 (1.802 - 3.054)	15.89 (12.31 - 20.53)	7.156 (5.021 - 10.07)	9.107 (7.122 - 11.58)	62.46 (56.43 - 69.54)	39.97 (32.63 - 49.84)
72h	0.5768 (0.4109 - 0.7963)	6.602 (4.310 - 9.753)	3.159 (2.213 - 4.391)	4.006 (3.189 - 4.957)	34.20 (28.56 - 41.32)	30.75 (25.95 - 36.68)

The LDH release assay was used to determine the cytotoxicity of Mito6_TPP, Mito6_picol. and Mito6_isoq. on COV434 cells. Cells were treated with the compounds in the lower concentrations that induced cell viability reduction (1-20 μM) and were evaluated after 48 hours of incubation. The results showed that Mito6_TPP at 10 μM and 20 μM and Mito6_isoq. at 20 μM are cytotoxic to COV434 cells, increasing the LDH release in at least 22%. (Figure 28).

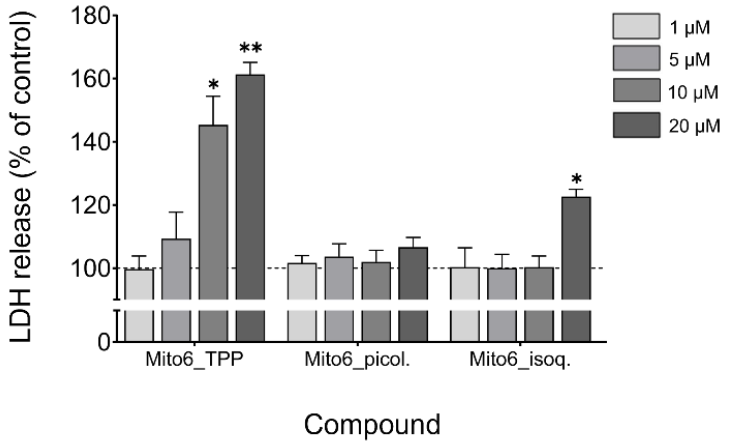

Figure 28 – Cytotoxicity of Mito6_TPP, Mito6_picol. or Mito6_isoq. (1-20 μM) in COV434 cells after 48h of incubation. Cytotoxicity assessed by LDH release assay. Untreated cells were used as control. Control is represented as a dotted line at 100%. Results are compared to the control and expressed as mean ± SEM of at least three independent experiments performed in triplicate. Significant differences between treated and untreated cells are described as * ($p<0,05$) and ** ($p<0,01$).

3.2. Mitochondrial membrane potential (Δψm)

The impact of Mito6_TPP, Mito6_picol. and Mito6_isoq. on COV434 cells' Δψm was assessed using a fluorescence assay with $DiOC_6$ probe. Cells were treated with the chosen concentration of each compound: 5 μM of Mito6_TPP, 20 μM of Mito6_picol. and 10 μM of Mito6_isoq. and the Δψm was evaluated at 48 hours of incubation. These concentrations were chosen for the same reasons as the other cell lines.

The experiments revealed that all compounds induced a Δψm decrease, and once again, Mito6_TPP was the most potent compound, inducing a decrease of 64% in Δψm with only a concentration of 5 μM (Figure 29).

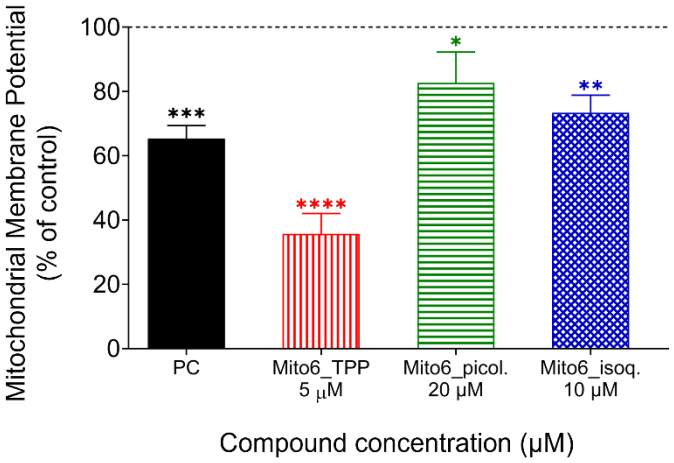

Figure 29 – Mitochondrial membrane potential of COV434 cells after 48h of incubation with 5 μM of Mito6_TPP, 20 μM of Mito6_picol. or 10 μM of Mito6_isoq. Δψm assessed by fluorescence assay with $DiOC_6$ probe. Untreated cells were used as control. CCCP (50 μM) was used as positive control (PC). Control is represented as a dotted line at 100%. Results are compared to the control and expressed as mean ± SEM of at least three independent experiments performed in triplicate. Significant differences between treated and untreated cells are described as * (p<0,05), ** (p<0,01), *** (p<0,001) and **** (p<0,0001).

3.3. Cell morphology

To examine the morphological changes that might be induced by the compounds, COV434 cells were directly observed under a phase contrast microscope or stained with either Giemsa or Höechst first. Cells were treated with the chosen concentration of every compound: 5 μM of Mito6_TPP, 20 μM of Mito6_picol. and 10 μM of Mito6_isoq. and observed after 48 hours of incubation. These concentrations were chosen for the same reasons as the other cell lines.

The images shown in Figure 30 were considered to be representative of all assays. The results showed that Mito6_TPP was the compound that induced more changes: in the phase contrast microscopy and Giemsa staining, a clear reduction in cell density was visible, as well as alterations in the shape of the cells and their nucleus. In Giemsa and Höechst staining it was possible to see signs of chromatin condensation, and even some nucleus fragmentation.

As observed in Figure 30, Mito6_picol. did not induce morphological changes in the cells, only a decrease in cell density was visible.

Mito6_isoq. was one more time the second most potent compound, inducing some morphological changes: in the phase contrast microscopy and Giemsa staining, a small reduction in cell density and an altered shape of the cell was noticeable and in Giemsa

staining and Höechst staining. In Höechst staining, there were a few signs of chromatin condensation with nucleus fragmentation (Figure 30).

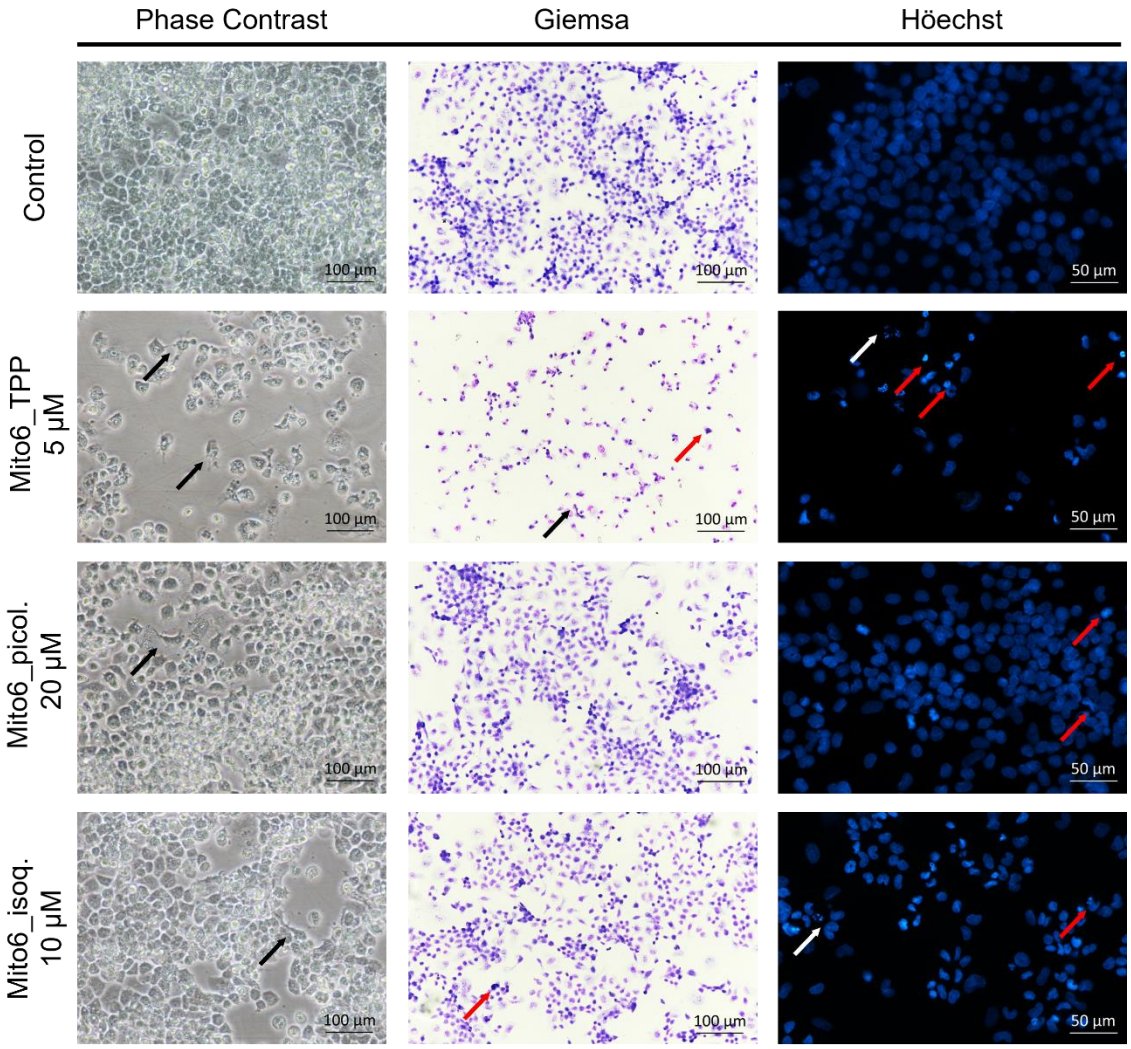

Figure 30 – Morphology of COV434 cells after 72h of incubation with 5 µM of Mito6_TPP, 20 µM of Mito6_picol. or 10 µM of Mito6_isoq. Morphology assessed by phase contrast, Giemsa and Höechst staining. Untreated cells were used as control. Black arrows indicate abnormal cell morphology; Red arrows indicate chromatin condensation; White arrows indicate nucleus fragmentation.

3.4. Intracellular reactive oxygen and nitrogen species (ROS/RNS) levels

The effects on ROS levels induced by Mito6_TPP, Mito6_picol. and Mito6_isoq. on COV434 cells were evaluated with a fluorescence assay with the DCFH-DA probe. Cells were treated with 10 µM of each compound only after incubation with the DCFH-DA. This concentration was chosen for the same reason as the other cell lines. ROS release was then evaluated every 5 minutes for 2 hours immediately after treatment.

The results showed that only Mito6_TPP was able to induce a decrease in ROS release that was significant starting at 65 minutes and reaching only 79% of the control at the end of the 2h of incubation (Figure 31).

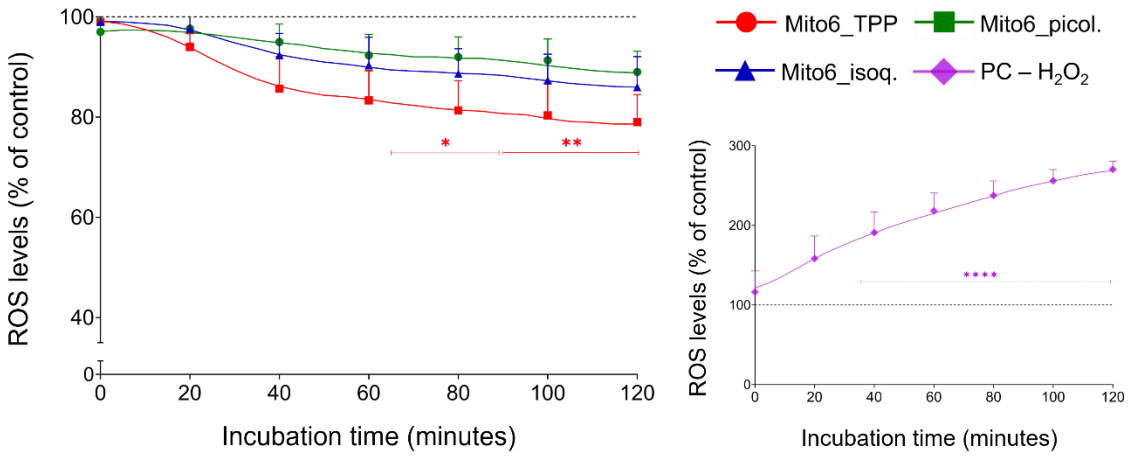

Figure 31 – Intracellular ROS levels by COV434 cells in the 2h immediately after the addition of 10 μM of Mito6_TPP, Mito6_picol. or Mito6_isoq. Left: ROS release assessed by fluorescence assay with DCFH-DA probe. Untreated cells were used as control. **Right:** H_2O_2 (200 μM) was used as positive control. Control is represented as a dotted line at 100%. Results are compared to the control and expressed as mean of at least three independent experiments performed in triplicate. Significant differences between treated and untreated cells are described as * (p<0,05) and ** (p<0,01).

3.5. Cleaved PARP-1 expression

A Western Blot was performed to explore the expression of cleaved PARP-1 in COV434 cells treated with 5 μM of Mito6_TPP, 20 μM of Mito6_picol. and 10 μM of Mito6_isoq. for 72h. Although preliminary, the results suggested that 5 μM of Mito6_TPP induced an increase in cleaved PARP-1 expression. On the other hand, the other compounds did not have the same effects in COV434 cells (Figure 32).

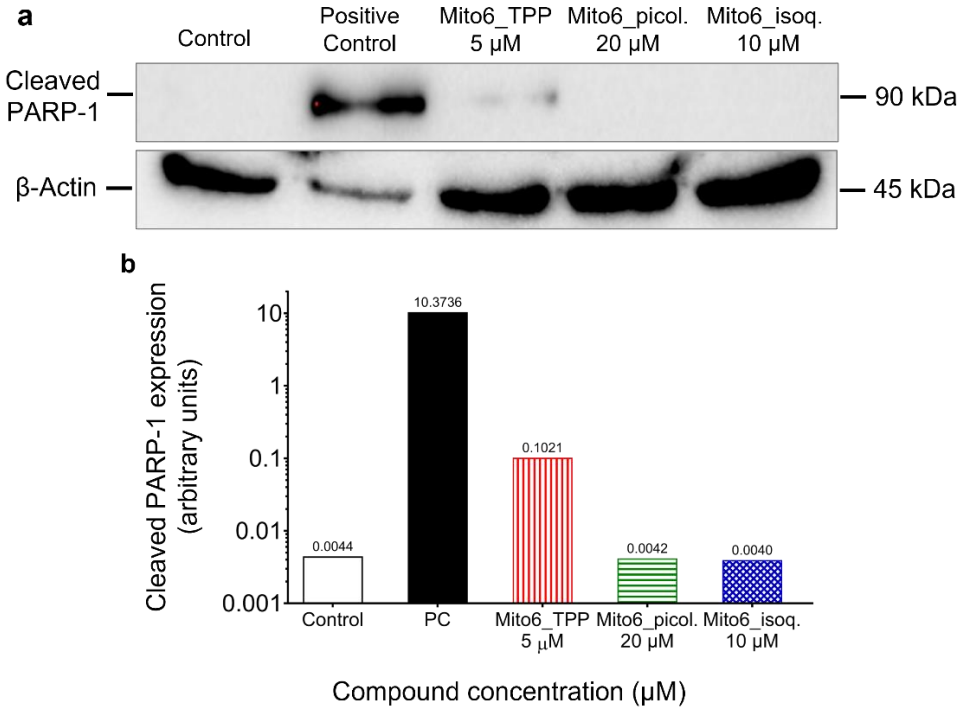

Figure 32 – Cleaved PARP-1 expression by COV434 after 72h of incubation with 5 μM of Mito6_TPP, 20 μM of Mito6_picol. or 10 μM of Mito6_isoq. Cleaved PARP-1 expression assessed by Western blot (a) and analyzed using Image Lab software from Bio Rad (b). Untreated cells were used as control. Staurosporine (10 μM) was used as positive control (PC). Results are expressed in arbitrary units of an isolated experiment, being only preliminary results.

4. HFF-1 cell line

4.1. Cell viability and cytotoxicity

The MTT and the Neutral Red assays were performed with the aim to investigate the effects of Mito6_TPP, Mito6_picol. and Mito6_isoq. on HFF-1 cell viability. Cells were treated with all the compounds in different concentrations ranging from 0.01 μM to 100 μM and its viability was evaluated at 24, 48 or 72 hours of incubation.

As observed in Figure 33, at 24h of incubation none of the compounds showed to induce any significant differences in cell viability.

At 48h, 100 μM of Mito6_TPP showed to induce a significant decrease of cell viability in MTT and NR assay. Mito6_isoq. at 100 μM also decreased cell viability using the MTT assay.

At 72h, Mito6_TPP induced reduction in cell viability in concentrations superior to 20 μM in the MTT assay and 50 μM in the NR assay. Mito6_picol. only induced reduction at 100 μM in NR assay. And Mito6_isoq. showed to induce effects at 100 μM in both assays (Figure 33).

The EC50 of Mito6_TPP, Mito6_picol. and Mito6_isoq. in HFF-1 cells was calculated in GraphPad Prism with the cell viability values obtained through the MTT assay and the NR assay in the graphics from Figure 33. The results showed that Mito6_TPP was the most effective compound, however, the lower EC50 was 37 μM which is higher than any of the concentrations chosen for further studies. The second most potent compound was Mito6_isoq. and lastly Mito6_picol., which had so little effect that it was not possible to calculate the EC50 rigorously in the MTT assay. Overall, none of the EC50 here obtained are comparable to the ones obtained with the tumor cell lines as these ones are much higher values, implying that the compounds need a much higher concentration to affect these cells. In this cell line, the NR assay allowed to obtain lower values of EC50 than the MTT assay (Table 6).

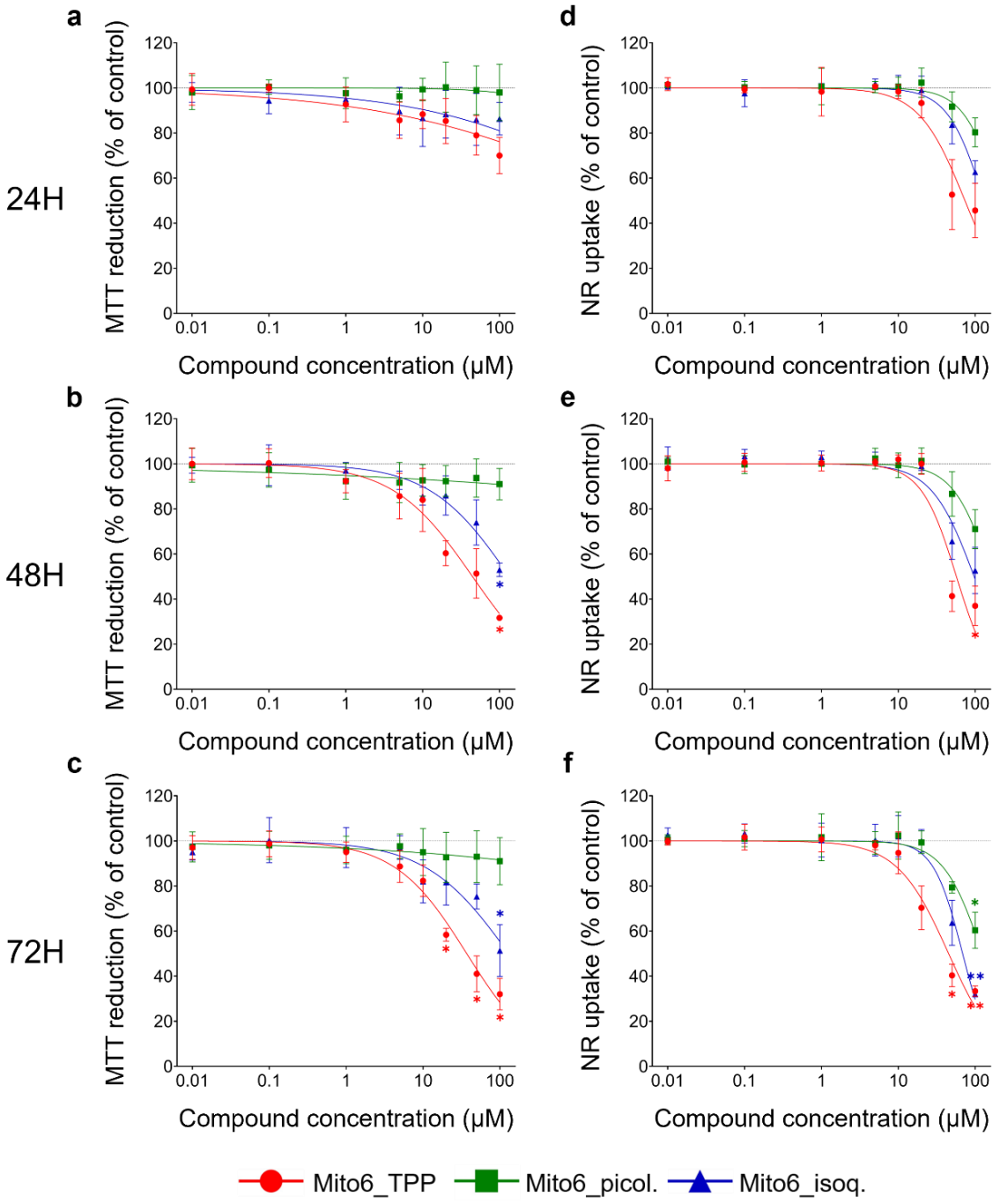

Figure 33 – Viability of HFF-1 cells treated with Mito6_TPP, Mito6_picol. or Mito6_isoq. (0,01-100 μM) at 24h, 48h and 72h of incubation. Viability assessed by MTT assay (a, b, c) and NR assay (d, e, f). Untreated cells were used as control. Control is represented as a dotted line at 100%. Results are compared to the control and expressed as mean ± SEM of at least three independent experiments performed in triplicate. Significant differences between treated and untreated cells are described as * ($p<0,05$) and ** ($p<0,01$).

Table 6 – EC50 of Mito6_TPP, Mito6_picol. and Mito6_isoq. in HFF-1 cells at 24h, 48h, 72h of incubation. The values were calculated by GraphPad Prism using the decrease of viability obtained through the MTT or the NR assay. [1]CI: Confidence Interval at 95%.

	EC50 (μM) – Mean (CI 95%)[1]					
	MTT assay			NR assay		
	Mito6_TPP	Mito6_picol.	Mito6_isoq.	Mito6_TPP	Mito6_picol.	Mito6_isoq.
24h	>100 ---	>100 ---	>100 ---	73.62 (59.20 - 96.85)	>100 ---	>100 ---
48h	44.54 (34.53 - 59.93)	>100 ---	>100 ---	56.98 (47.18 - 70.11)	>100 ---	96.96 (81.95 - 121.3)
72h	37.04 (30.84 - 45.14)	>100 ---	>100 ---	45.10 (38.10 - 53.97)	>100 ---	68.64 (64.43 - 77.04)

The LDH release assay was not performed in this cell line due to the lack of significant cell viability decrease at the concentrations tested in the other cell lines.

4.2. Mitochondrial membrane potential (Δψm)

To evaluate the influence of Mito6_TPP, Mito6_picol. and Mito6_isoq. on Δψm in HFF-1 cells, it was used a fluorescence assay with the $DiOC_6$ probe. Cells were treated with the chosen concentration of each compound: 5 μM of Mito6_TPP, 20 μM of Mito6_picol. and 10 μM of Mito6_isoq. and evaluated at 48 hours of incubation. These concentrations are the same as used in the other cell lines as this cell line is used as control.

The results showed that none of the compounds induced a significant decrease in Δψm in HFF-1 healthy cells (Figure 34).

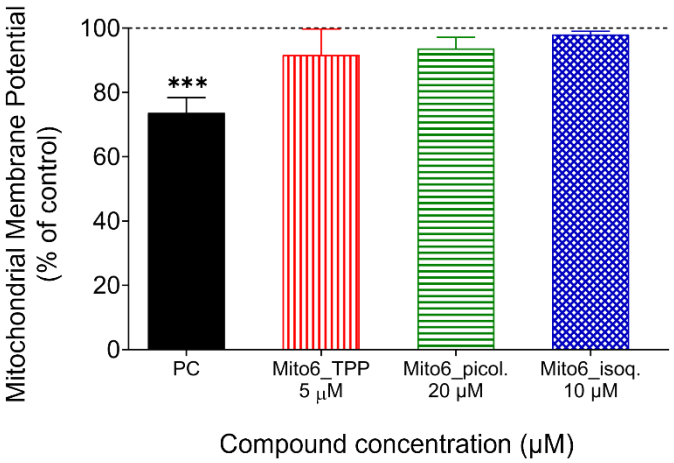

Figure 34 – Mitochondrial membrane potential of HFF-1 cells after 48h of incubation with 5 μM of Mito6_TPP, 20 μM of Mito6_picol. or 10 μM of Mito6_isoq. Δψm assessed by fluorescence assay with $DiOC_6$ probe. Untreated cells were used as control. CCCP (50 μM) was used as positive control (PC). Control is represented as a dotted line at 100%. Results are compared to the control and expressed as mean ± SEM of at least three independent experiments performed in triplicate. Significant differences between treated and untreated cells are described as *** (p<0,001).

4.3. Cell morphology

Morphological changes in HFF-1 cells derived from the incubation with Mito6_TPP, Mito6_picol. and Mito6_isoq. were directly evaluated under a phase contrast microscope or first stained with Giemsa. Höechst staining was not performed in this cell line due to a lack of indications of apoptosis. Cells were treated with the tested concentration of 5 µM, 20 µM and 10 µM for Mito6_TPP, Mito6_picol. and Mito6_isoq., respectively, and observed after 72 hours of incubation. These concentrations are the same as used in the other cell lines as this cell line is used as control.

The images shown in Figure 35 were considered to be representative of all assays. In the concentrations tested, none of the compounds showed to induce any differences in cellular morphology of HFF-1 cells.

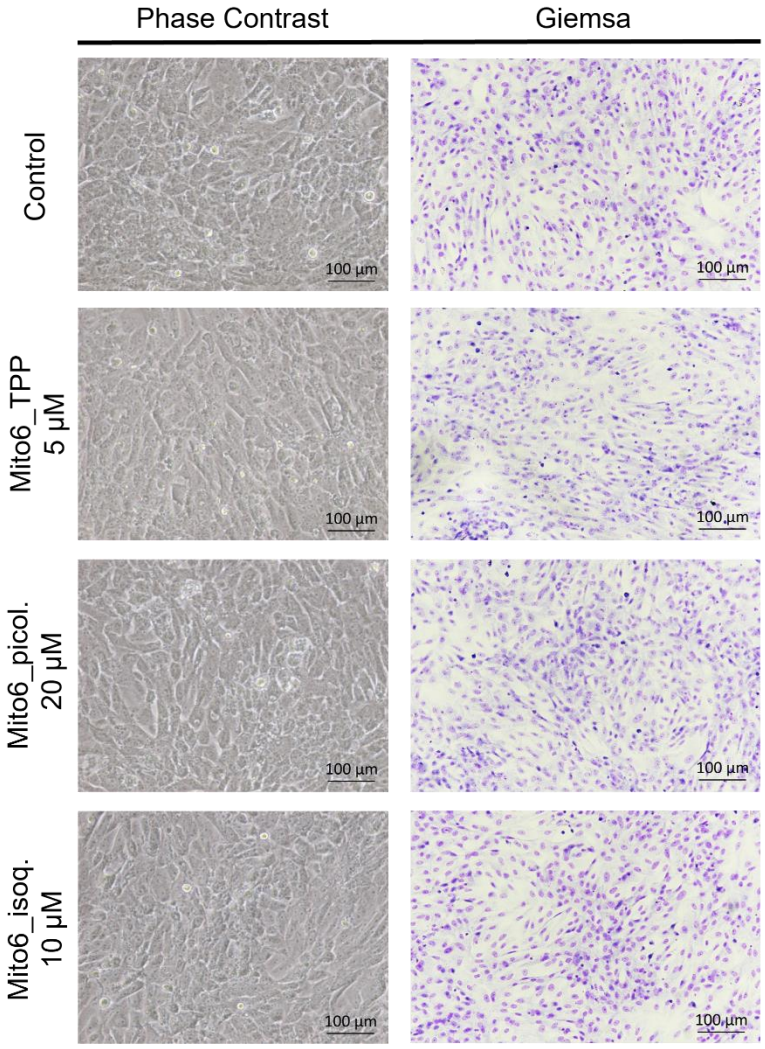

Figure 35 – Morphology of HFF-1 cells after 72h of incubation with 5 µM of Mito6_TPP, 20 µM of Mito6_picol. or 10 µM of Mito6_isoq. Morphology assessed by phase contrast and Giemsa. Untreated cells were used as control.

4.4. Intracellular reactive oxygen and nitrogen species (ROS/RNS) levels

A fluorescence assay with DCFH-DA was performed to assess the effects of Mito6_TPP, Mito6_picol. and Mito6_isoq. on HFF-1 cells' ROS release. Cells were incubated with DCFH-DA for an hour, and then 10 μM of each compound were added. This concentration is the same as used in the other cell lines as this cell line is used as control. ROS release was measured for 2 hours immediately after treatment with the compounds.

Results showed that none of the compounds was able to induce significant alterations in the ROS release in the healthy HFF-1 cells (Figure 36).

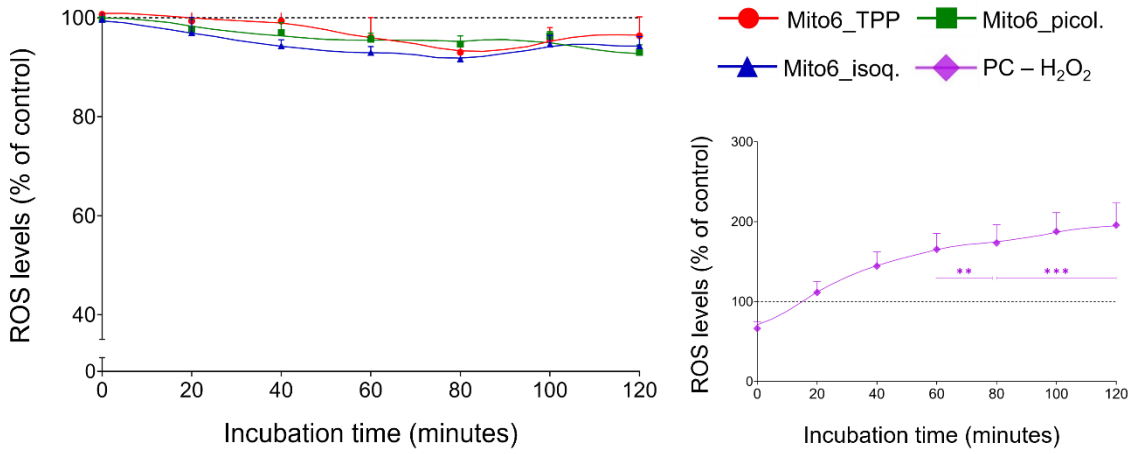

Figure 36 – Intracellular ROS levels by HFF-1 cells in the 2h immediately after the addition of 10 μM of Mito6_TPP, Mito6_picol. or Mito6_isoq. Left: ROS release assessed by fluorescence assay with DCFH-DA probe. Untreated cells were used as control. **Right:** H_2O_2 (200 μM) was used as positive control. Control is represented as a dotted line at 100%. Results are compared to the control and expressed as mean of at least three independent experiments performed in triplicate. No significant differences between treated and untreated cells were detected.

Discussion and conclusion

Ovarian and endometrial cancers are among the most lethal types of cancer in women. Its incidence mainly affects industrialized countries. Late diagnosis is one of the factors that contributes to poor prognosis together with the lack of targeted drugs that can effectively combat these pathologies. Mitocans emerged to try to find effective compounds that can target tumor cells and destroy them. In particular, TPP-based mitocans have shown promising results in terms of specificity and efficacy. For example, Gazzano, E. *et al.* found in 2018 that two phenolic esters TPP-derivatives had cytotoxic properties against colon, lung and breast cancer cell lines, and did not show toxicity against normal cells[78]. TPP-based mitocans are also being studied as a potent strategy to overcome drug resistance. Han, M. *et al.* added a TPP moiety to doxorubicin to try to overcome doxorubicin resistance in cancer cells and discovered that the conjugate was taken up at a higher rate than the free doxorubicin[79]. Millard, M. et al. successfully used a TPP-chlorambucil conjugate to overcome insensitivity to chlorambucil in breast and pancreatic cancer cell lines[80].

Other lipophilic cations, such as 4-picoline or isoquinoline, have also been studied in order to achieve the same therapeutical effect. In this work, several experiments were performed in different cell lines to test the efficacy and specificity for tumor cells of three antioxidants based on the caffeic acid containing different transport cation carries.

Regarding cell viability assays, it is clear that Mito6_TPP was the most effective and selective of all tested compounds, as it affected tumor cells more than the control cells. This compound was able to induce a significant decrease in cell viability at concentrations as low as 1 μM in Ishikawa and COV434 and 5 μM in Hec50co cells. Moreover, in HFF-1 cells, used as a control, only concentrations above 20 μM were able to induce a reduction in cell viability. These assays confirmed the theory that the TPP cation can accumulate more in tumor cells than in healthy cells. Concerning cytotoxicity of this compound, it induced significant cell lysis only at concentrations above 10 μM in COV434 and 20 μM in Ishikawa. In turn, no effects were observed in Hec50co cells. In addition, COV434 was the cell line that was most affected by this compound, suffering its effects at low concentrations and in short times of incubation. Interestingly, the Hec50co cell line was the most resistant to the effects of Mito6_TPP.

Mito6_isoq. induced significant reduction in cell viability at concentrations superior to 10 μM in Ishikawa cells, 5 μM in Hec50co and 1 μM in COV434, while in HFF-1 cells it was necessary to have 100 μM of compound to induce any effects. Regarding cytotoxicity of Mito6_isoq., it only showed to be cytotoxic at 20 μM in COV434 cells. In this case,

COV434 was again the most affected cell line. However, Hec50co was not the less sensitive cell line this time, as Ishikawa cells needed higher concentrations of Mito6_isoq. to suffer reduction of cell viability. In general, Mito6_isoq. did not have the same potency as Mito6_TPP, however, it was selective and only affected healthy cells in the highest concentrations tested.

The least effective compound was Mito6_picol. It induced a reduction in cell viability at 20 μM in Ishikawa, 10 μM in Hec50co and 1 μM in COV434 cells, whereas in HFF-1 cells, it only induced decrease in cell viability at 100 μM. Regarding the cytotoxicity assay, Mito6_picol. did not show to be cytotoxic at any concentration tested in any cell line. Moreover, COV434 was the most sensitive cell line, followed by Hec50co and the most resistant cell line was Ishikawa. This compound needed higher concentrations to induce effects on tumor cell lines, nevertheless, it was selective and did not affect healthy cells except at the highest concentrations tested.

The calculations of the EC50 showed that the MTT and the NR assay had different sensitivities regardless of the detection of viable cells. Overall, the MTT assay allowed to obtain lower values of EC50 than the NR assay on tumor cell lines. Surprisingly, in HFF-1 cells, contrary to tumor cells, the NR assay allowed to obtain lower values than the MTT assay. It is also important to reaffirm that the values of EC50 obtained for the tumor cell lines are very low compared to the values obtained for the control cell line, confirming the selectivity of the compounds. However, none of the assays is perfect for determining the accurate EC50. These inconsistencies are due to the different types of cells used, as their metabolism is different and therefore, they will metabolize the MTT and the NR in different ways. That is why the use of more than one assay to determine cell viability is recommended.

Overall, COV434 was the most affected cell line by all the compounds. Between Ishikawa and Hec50co, the most sensitive cell line depends on the compound and the incubation time. These different effects caused by the compounds in each cell line do not have a simple explanation that can be based on these results. However, the different metabolisms and proliferation rates of the cells might accelerate or retardate the effects that the compounds cause. For example, Hec50co and Ishikawa cells present a much higher proliferation rate and are less affected by the compounds than COV434. This might be because Hec50co and Ishikawa are reproducing fast and are not allowing enough time for the compounds to act in all cells, stopping their proliferation. On the contrary, as COV434 reproduce slower, the compounds have time to act in the existent cells to stop their proliferation.

The control cells HFF-1 did not suffer any effect of the compounds at 24h and only 100 μM of Mito6_TPP and Mito6_isoq. at 48h of incubation were able to cause significant cell viability decrease. However, at 72h of incubation in HFF-1 cells, 20 μM of Mito6_TPP already induced a reduction in cell viability while Mito6_isoq. and Mito6_picol still needed 100 μM. This data is important as it shows that depending on the incubation time, Mito6_TPP might be too aggressive to healthy cells contrary to Mito6_isoq. and Mito6_picol.

The defined concentrations for each compound (5 μM of Mito6_TPP, 10 μM of Mito6_isoq. and 20 μM of Mito6_picol.) were used to further explore the role of these compounds in cell death. As at these concentrations, there was a decrease in cell viability, but the compounds did not show signs of cytotoxicity, there is an indication that the cells are selectively dying, which may suggest apoptosis. To explore these signs, an assay that evaluated the Δψm was performed, as the decrease in the Δψm is one of the conditions of the intrinsic apoptosis pathway. Mito6_TPP and Mito6_isoq. were both able to induce a significant decrease in the Δψm compared to untreated cells in all tumor cell lines, although Mito6_TPP produced more drastic effects. Mito6_picol. induced a decrease in Δψm in Ishikawa and COV434 cells, but was not able to produce effects in Hec50co cells. These Δψm measurement results support the hypothesis that apoptosis may be the type of cell death that occurs at the tested concentrations of the compounds. Regarding the HFF-1 cells, none of the compounds induced differences in Δψm comparing to untreated cells.

Another element that supports the findings previously described is the study of cell morphology. Mito6_TPP and Mito6_isoq. induced a significant morphological change, as all tumor cell lines showed altered shape of the cell and its nucleus and presented signs of chromatin condensation. Moreover, Ishikawa and COV434 cells also showed nuclear fragmentation in Höechst staining, when incubating with Mito6_TPP. Mito6_picol. did not induce any morphological changes in any tumor cell line. These findings support the fact that the most potent compound tested was Mito6_TPP. They also support the fact that apoptosis may be present, as chromatin condensation is a step in the apoptosis process and nucleus fragmentation is a consequence of this. Regarding HFF-1 cells, none of the compounds induced changes in their morphology.

To try to confirm the apoptosis hypothesis, the expression of cleaved PARP-1 was explored, as it is a substrate for essential proteases with roles in the apoptosis process, such as caspases. This assay was performed for the first time in COV434, as these cells were the ones that showed to be more sensitive to the compounds. However, the same assay should be performed for the other tumor cell lines. The results are only preliminary,

as the test was not repeated to confirm it; however, the current result demonstrates that incubation with Mito6_TPP for 48h indeed induced an increase in the expression of cleaved PARP, indicating apoptosis. When incubated with the other compounds, no effect was visible, implying that, at that concentration and incubation time, Mito6_isoq. and Mito6_picol did not induce apoptosis in COV434 cells.

Although the cell viability is decreasing and the most normal scenario, in this case, is the ROS increase, the three compounds here used have antioxidant properties. Therefore, free ROS were also measured to assess the effects of the compounds in the cells. In general, the compounds induced a decrease in the ROS levels, due to their antioxidant properties. Mito6_TPP was the compound that induced the most effective and fast decrease in ROS release in all tumor cell lines, followed by Mito6_isoq. and Mito6_picol. that induce no effects on COV434 cells. This result supports the other findings implying that Mito6_TPP was the most potent compound that affected all tumor cell lines. Surprisingly, COV434 was the least affected cell line in terms of free ROS, probably due to the fact that 10 μM is a concentration that already induces cell death and shows some cytotoxicity, therefore, the mechanism of death present might be unspecified. Ishikawa and Hec50co both suffered a decrease in ROS when incubating with all the compounds, however, Ishikawa cells were the most sensitive. HFF-1 healthy cells did not suffer any effect in intracellular ROS when incubated with all compounds.

As all compounds have antioxidant properties, the results of the ROS measurement are according to expected. However, the mechanism of delivery of the compounds is dependent on the cation carrier, with TPP being considered the most potent of the three cations tested. Moreover, this drastic decrease in intracellular ROS might be one of the reasons that the cell viability is decreasing as cells are losing the necessary quantity of ROS they need to keep their normal signaling processes and will stop proliferating. In other words, treatment with antioxidants in tumor cells will induce decrease in ROS levels and cells will not have enough to maintain their growth. However, the mechanism used by the compounds to reduce intracellular ROS is not known: it may be a simple redox reaction as the compound may directly interact with the species or the compound may be inhibiting one of the enzymes responsible for the ROS chain production.

It is now clear that Mito6_picol. does not have the same potency to destroy tumor cells as the other two compounds. However, it is not clear whether it is Mito6_TPP or Mito6_isoq. which brings the most interesting set of advantages and disadvantages. Mito6_TPP has been shown to be extremely effective, dramatically reducing cell viability in all cell lines, even at low incubation times. The cytotoxicity problem associated with Mito6_TPP has already been described by Benfeito, S. *et al.* and was attributed to the

presence of the TPP moiety together with the length of the linker that increases the hydrophobicity of the compound. The authors suggested that the substitution of the TPP moiety for isoquinoline or 4-picoline could prevent the cytotoxicity[67]. As suggested, the substitution of TPP for isoquinoline or 4-picoline indeed prevented the cytotoxicity of the compound, which is one of the main advantages of Mito6_isoq. Although it needs more incubation time to achieve the same effects that Mito6_TPP can produce, it is capable of producing the same consequences and has the advantage that only concentrations above 100 μM were able to induce any changes in healthy cells.

Different cells have different characteristics and metabolic pathways that will affect their response to the input of the compounds differently. In this case, mitochondria-related metabolism and membrane potentials are some of the most important cellular characteristics that can influence the effect of the compounds. Due to this, the effects of the compounds on the three tumor cell lines were different: COV434 were affected by all compounds to different extents, but always requiring a small concentration of the compound. On the contrary, Ishikawa and Hec50co were more affected by Mito6_TPP and Mito6_isoq. as it was necessary to have a high concentration of Mito6_picol. to produce the same effect. On the other hand, HFF-1 cells always needed a higher concentration of compounds to feel any effects, which proves that the three compounds had a greater tendency to attack tumor cells instead of attacking all cells indiscriminately.

It is unclear if at the intermediate concentrations tested the cells are indeed dying in a controlled manner and suffering apoptosis. Although these results provide good indications of that, more studies are necessary to prove it, for example, the Western Blot for cleaved PARP-1 in COV434 has to be repeated to confirm and must be reproduced for the other cell lines. It is also necessary to unravel the mechanism of action of these compounds to figure out exactly how and where they act in the cell, and the fact that they decrease free intracellular ROS is a starting point to start these types of studies. The assays contained in this work can also be performed on other types of tumor cells as Mito6_TPP and Mito6_isoq. show anticancer potential in all tumor cell lines tested.

Besides, more tests on healthy cells should be performed to ensure the selectivity of these compounds for tumor cells only, and that the compounds can be metabolized when necessary. If future assays continue to indicate that these compounds have potential, further studies in animals may be the next step.

Overall, this study supports the emergence of mitocans and, in particular, TPP-based mitocans as a new category of anticancer agents. They have the potential to improve current therapies used to combat these pathologies. The assays performed here indicate

the potential that the tested antioxidants have to combat tumors, in particular, GC and endometrial tumors of type 1 and 2, without affecting normal cells. Of the three compounds tested, Mito6_TPP demonstrated to be the most potent, Mito6_isoq. can exert the same effects as Mito6_TPP if more time is given without being toxic to normal cells and Mito6_picol. has some effects although they are less significant. Although the mechanisms underlying the effects of these compounds need to be deeply studied, this study provides information that supports the potential these compounds have to combat GC and endometrial tumors without affecting normal cells.

References

1. Hawkins, S. M.; Matzuk, M. M., The menstrual cycle: basic biology. *Ann. N. Y. Acad. Sci.* **2008,** *1135*, 10-8. doi: 10.1196/annals.1429.018

2. Jones, R. E.; Lopez, K. H., *Chapter 3 - The Menstrual Cycle*. In *Human Reproductive Biology (Fourth Edition)*, Jones, R. E.; Lopez, K. H., Eds. Academic Press: San Diego; 2014; 51-66, ISBN: 978-0-12-382184-3

3. Rodgers, R. J.; Irving-Rodgers, H. F., Formation of the ovarian follicular antrum and follicular fluid. *Biol. Reprod.* **2010,** *82* (6), 1021-9. doi: 10.1095/biolreprod.109.082941

4. Richards, J. S., The Ovarian Cycle. *Vitam. Horm.* **2018,** *107*, 1-25. doi: 10.1016/bs.vh.2018.01.009

5. Vainio, S. J.; Pelliniemi, L. J.; Ritvos, D. O., *Development of the adreno-genital system*; 2002; ISBN: 951-42-6843-1

6. Maybin, J. A.; Critchley, H. O. D., Menstrual physiology: implications for endometrial pathology and beyond. *Hum. Reprod. Update* **2015,** *21* (6), 748-761. doi: 10.1093/humupd/dmv038

7. Myers, K. M.; Elad, D., Biomechanics of the human uterus. *Wiley Interdiscip. Rev. Syst. Biol. Med.* **2017,** *9* (5). doi: 10.1002/wsbm.1388

8. Aitken, R. J.; Baker, M. A.; Doncel, G. F.; Matzuk, M. M.; Mauck, C. K.; Harper, M. J. K., As the world grows: contraception in the 21st century. *J. Clin. Investig.* **2008,** *118* (4), 1330-1343. doi: 10.1172/JCI33873

9. Silva, J. F.; Ocarino, N. M.; Serakides, R., Thyroid hormones and female reproduction. *Biol. Reprod.* **2018,** *99* (5), 907-921. doi: 10.1093/biolre/ioy115

10. Christensen, A.; Bentley, G. E.; Cabrera, R.; Ortega, H. H.; Perfito, N.; Wu, T. J.; Micevych, P., Hormonal regulation of female reproduction. *Horm. Metab. Res.* **2012,** *44* (8), 587-91. doi: 10.1055/s-0032-1306301

11. Bray, F.; Ferlay, J.; Soerjomataram, I.; Siegel, R. L.; Torre, L. A.; Jemal, A., Global cancer statistics 2018: GLOBOCAN estimates of incidence and mortality worldwide for 36 cancers in 185 countries. *CA: Cancer J. Clin.* **2018,** *68* (6), 394-424. doi: 10.3322/caac.21492

12. Ferlay J, L. M., Ervik M, Lam F, Colombet M, Mery L, Piñeros M, Znaor A, Soerjomataram I, Bray F, *Global Cancer Observatory: Cancer Tomorrow* (accessed 21 December 2020).

13. Hunn, J.; Rodriguez, G. C., Ovarian Cancer: Etiology, Risk Factors, and Epidemiology. *Clin. Obstet. Gynecol.* **2012,** *55* (1). doi: 10.1097/grf.0b013e31824b4611

14. Prat, J.; Espinosa, I.; D'Angelo, E., *Ovarian Cancer: Pathology and Genetics.* In *Encyclopedia of Cancer (Third Edition)*, Boffetta, P.; Hainaut, P., Eds. Academic Press: Oxford; 2019; ISBN: 978-0-12-812485-7

15. Stewart, C.; Ralyea, C.; Lockwood, S., Ovarian Cancer: An Integrated Review. *Semin. Oncol. Nurs.* **2019,** *35* (2), 151-156. doi: 10.1016/j.soncn.2019.02.001

16. Goff, B., Symptoms associated with ovarian cancer. *Clin. Obstet. Gynecol.* **2012,** *55* (1), 36-42. doi: 10.1097/GRF.0b013e3182480523

17. Bhosale, P.; Kamat, A.; Eifel, P. J., *Chapter 26 - Ovarian Cancer*. In *Oncologic Imaging: A Multidisciplinary Approach*, Silverman, P. M., Ed. W.B. Saunders: Philadelphia; 2012; ISBN: 978-1-4377-2232-1

18. DeFriend, D., *CHAPTER 35 - Ovaries*. In *Clinical Ultrasound (Third Edition)*, Allan, P. L.; Baxter, G. M.; Weston, M. J., Eds. Churchill Livingstone: Edinburgh; 2011; ISBN: 978-0-7020-3131-1

19. Brodniewicz, T.; Grynkiewicz, G., Preclinical drug development. *Acta Pol. Pharm.* **2010,** *67* (6), 578-85.

20. Zhang, H.; Vollmer, M.; De Geyter, M.; Litzistorf, Y.; Ladewig, A.; Dürrenberger, M.; Guggenheim, R.; Miny, P.; Holzgreve, W.; De Geyter, C., Characterization of an immortalized human granulosa cell line (COV434). *Mol. Hum. Reprod.* **2000,** *6* (2), 146-53. doi: 10.1093/molehr/6.2.146

21. Zhang, S.; Gong, T.-T.; Liu, F.-H.; Jiang, Y.-T.; Sun, H.; Ma, X.-X.; Zhao, Y.-H.; Wu, Q.-J., Global, Regional, and National Burden of Endometrial Cancer, 1990-2017: Results From the Global Burden of Disease Study, 2017. *Front. Oncol.* **2019,** *9*, 1440-1440. doi: 10.3389/fonc.2019.01440

22. Colombo, N.; Preti, E.; Landoni, F.; Carinelli, S.; Colombo, A.; Marini, C.; Sessa, C., Endometrial cancer: ESMO Clinical Practice Guidelines for diagnosis, treatment and follow-up†. *Ann. Oncol.* **2013,** *24*, vi33-vi38. doi: 10.1093/annonc/mdt353

23. Shai, A.; Segev, Y.; Narod, S. A., Genetics of endometrial cancer. *Fam. Cancer* **2014,** *13* (3), 499-505. doi: 10.1007/s10689-014-9722-7

24. Braun, M. M.; Overbeek-Wager, E. A.; Grumbo, R. J., Diagnosis and Management of Endometrial Cancer. *Am. Fam. Physician* **2016,** *93* (6), 468-74.

25. Pakish, J. B.; Lu, K. H.; Sun, C. C.; Burzawa, J. K.; Greisinger, A.; Smith, F. A.; Fellman, B.; Urbauer, D. L.; Soliman, P. T., Endometrial Cancer Associated Symptoms: A Case-Control Study. *J. Women's Health* **2016,** *25* (11), 1187-1192. doi: 10.1089/jwh.2015.5657

26. Ryan, A.; Susil, B.; Jobling, T.; Oehler, M., Endometrial cancer. *Cell Tissue Res.* **2005,** *322*, 53-61. doi: 10.1007/s00441-005-1109-5

27. Otify, M.; Fuller, J.; Ross, J.; Shaikh, H.; Johns, J., Endometrial pathology in the postmenopausal woman – an evidence based approach to management. *Obstet. Gynecol.* **2014,** *17*. doi: 10.1111/tog.12150

28. Castelbaum, A. J.; Ying, L.; Somkuti, S. G.; Sun, J.; Ilesanmi, A. O.; Lessey, B. A., Characterization of integrin expression in a well differentiated endometrial adenocarcinoma cell line (Ishikawa). *J. Clin. Endocrinol. Metab.* **1997,** *82* (1), 136-42. doi: 10.1210/jcem.82.1.3658

29. Nishida, M., The Ishikawa cells from birth to the present. *Hum. Cell* **2002,** *15* (3), 104-117. doi: 10.1111/j.1749-0774.2002.tb00105.x

30. Albitar, L.; Pickett, G.; Morgan, M.; Davies, S.; Leslie, K. K., Models representing type I and type II human endometrial cancers: Ishikawa H and Hec50co cells. *Gynecol. Oncol.* **2007,** *106* (1), 52-64. doi: 10.1016/j.ygyno.2007.02.033

31. Olgen, S., Overview on Anticancer Drug Design and Development. *Curr. Med. Chem.* **2018,** *25* (15), 1704-1719. doi: 10.2174/0929867325666171129215610

32. Winkler, G. C.; Barle, E. L.; Galati, G.; Kluwe, W. M., Functional differentiation of cytotoxic cancer drugs and targeted cancer therapeutics. *Regul. Toxicol. Pharmacol.* **2014,** *70* (1), 46-53. doi: 10.1016/j.yrtph.2014.06.012

33. Sun, J.; Wei, Q.; Zhou, Y.; Wang, J.; Liu, Q.; Xu, H., A systematic analysis of FDA-approved anticancer drugs. *BMC Syst. Biol.* **2017,** *11* (5), 87. doi: 10.1186/s12918-017-0464-7

34. Siddiqui, N.; Ahsan, W.; Alam, M.; Andalip; Azad, B.; Akhtar, M., Newer biologically active pyridines: A potential review. *Res. J. Pharm. Technol.* **2011,** *4*, 1918-1932.

35. Rahman, F. U.; Bhatti, M. Z.; Ali, A.; Duong, H. Q.; Zhang, Y.; Yang, B.; Koppireddi, S.; Lin, Y.; Wang, H.; Li, Z. T.; Zhang, D. W., Homo- and heteroleptic Pt(II) complexes of ONN donor hydrazone and 4-picoline: A synthetic, structural and detailed mechanistic anticancer investigation. *Eur. J. Med. Chem.* **2018,** *143*, 1039-1052. doi: 10.1016/j.ejmech.2017.11.044

36. Rahman, F. U.; Ali, A.; Guo, R.; Zhang, Y. C.; Wang, H.; Li, Z. T.; Zhang, D. W., Synthesis and anticancer activities of a novel class of mono- and di-metallic Pt(II)(salicylaldiminato)(DMSO or Picolino)Cl complexes. *Dalton Trans.* **2015,** *44* (5), 2166-75. doi: 10.1039/c4dt03018d

37. Gao, F.; Liu, H.; Li, L.; Guo, J.; Wang, Y.; Zhao, M.; Peng, S., Design, synthesis, and testing of an isoquinoline-3-carboxylic-based novel anti-tumor lead. *Bioorg. Med. Chem. Lett.* **2015,** *25* (20) , 4434-6. doi: 10.1016/j.bmcl.2015.09.014

38. Ding, D.; Guo, Y. R.; Wu, R. L.; Qi, W. Y.; Xu, H. M., Two new isoquinoline alkaloids from Scolopendra subspinipes mutilans induce cell cycle arrest and apoptosis in human glioma cancer U87 cells. *Fitoterapia* **2016,** *110*, 103-9. doi: 10.1016/j.fitote.2016.03.004

39. Check Hayden, E., Cancer complexity slows quest for cure. *Nature* **2008,** *455* (7210), 148. doi: 10.1038/455148a

40. Friedman, J. R.; Nunnari, J., Mitochondrial form and function. *Nature* **2014,** *505* (7483) , 335-43. doi: 10.1038/nature12985

41. Yang, Y.; Karakhanova, S.; Hartwig, W.; D'Haese, J. G.; Philippov, P. P.; Werner, J.; Bazhin, A. V., Mitochondria and Mitochondrial ROS in Cancer: Novel Targets for Anticancer Therapy. *J. Cell. Physiol.* **2016,** *231* (12) , 2570-81. doi: 10.1002/jcp.25349

42. Ralph, S. J.; Rodríguez-Enríquez, S.; Neuzil, J.; Saavedra, E.; Moreno-Sánchez, R., The causes of cancer revisited: "mitochondrial malignancy" and ROS-induced oncogenic transformation - why mitochondria are targets for cancer therapy. *Mol. Aspects Med.* **2010,** *31* (2), 145-70. doi: 10.1016/j.mam.2010.02.008

43. Galluzzi, L.; Morselli, E.; Kepp, O.; Vitale, I.; Rigoni, A.; Vacchelli, E.; Michaud, M.; Zischka, H.; Castedo, M.; Kroemer, G., Mitochondrial gateways to cancer. *Mol. Aspects Med.* **2010,** *31* (1), 1-20. doi: 10.1016/j.mam.2009.08.002

44. Liberti, M. V.; Locasale, J. W., The Warburg Effect: How Does it Benefit Cancer Cells? *Trends Biochem. Sci.* **2016,** *41* (3), 211-218. doi: 10.1016/j.tibs.2015.12.001

45. Porporato, P. E.; Filigheddu, N.; Pedro, J. M. B.-S.; Kroemer, G.; Galluzzi, L., Mitochondrial metabolism and cancer. *Cell Res.* **2018,** *28* (3), 265-280. doi: 10.1038/cr.2017.155

46. Paulo, J. O., *Mitochondria Remodeling in Cancer*. In *Mitochondrial biology and experimental therapeutics*, Dordrecht; 2018; ISBN: 978-3-319-73344-9

47. Neuzil, J.; Dong, L.-F.; Rohlena, J.; Truksa, J.; Ralph, S. J., Classification of mitocans, anti-cancer drugs acting on mitochondria. *Mitochondrion* **2013,** *13* (3), 199-208. doi: 10.1016/j.mito.2012.07.112

48. Ichim, G.; Tait, S. W. G., A fate worse than death: apoptosis as an oncogenic process. *Nat. Rev. Cancer.* **2016,** *16* (8), 539-548.doi: 10.1038/nrc.2016.58

49. Paulo, J. O., Mitocans: *Mitochondrially Targeted Anti-cancer Drugs*. In *Mitochondrial biology and experimental therapeutics* Dordrecht; 2018; ISBN: 978-3-319-73344-9

50. Dong, L.; Gopalan, V.; Holland, O.; Neuzil, J., Mitocans Revisited: Mitochondrial Targeting as Efficient Anti-Cancer Therapy. *Int. J. Mol. Sci.* **2020,** *21* (21) , 7941. doi: 10.3390/ijms21217941

51. Dong, L.; Neuzil, J., Targeting mitochondria as an anticancer strategy. *Cancer Commun.* **2019,** *39* (1), 63. doi: 10.1186/s40880-019-0412-6

52. Battogtokh, G.; Choi, Y. S.; Kang, D. S.; Park, S. J.; Shim, M. S.; Huh, K. M.; Cho, Y. Y.; Lee, J. Y.; Lee, H. S.; Kang, H. C., Mitochondria-targeting drug conjugates for cytotoxic, anti-oxidizing and sensing purposes: current strategies and future perspectives. *Acta Pharm. Sin. B* **2018,** *8* (6), 862-880. doi: 10.1016/j.apsb.2018.05.006

53. Zielonka, J.; Joseph, J.; Sikora, A.; Hardy, M.; Ouari, O.; Vasquez-Vivar, J.; Cheng, G.; Lopez, M.; Kalyanaraman, B., Mitochondria-Targeted Triphenylphosphonium-Based Compounds: Syntheses, Mechanisms of Action, and Therapeutic and Diagnostic Applications. *Chem. Rev.* **2017,** *117* (15) , 10043-10120. doi: 10.1021/acs.chemrev.7b00042

54. Wang, J.; Li, J.; Xiao, Y.; Fu, B.; Qin, Z., TPP-based mitocans: a potent strategy for anticancer drug design. *RSC Med. Chem.* **2020,** *11* (8), 858-875. doi: 10.1039/C9MD00572B

55. Wang, J. Y.; Li, J. Q.; Xiao, Y. M.; Fu, B.; Qin, Z. H., Triphenylphosphonium (TPP)-Based Antioxidants: A New Perspective on Antioxidant Design. *ChemMedChem* **2020,** *15* (5), 404-410. doi: 10.1002/cmdc.201900695

56. Sandoval-Acuña, C.; Fuentes-Retamal, S.; Guzmán-Rivera, D.; Peredo-Silva, L.; Madrid-Rojas, M.; Rebolledo, S.; Castro-Castillo, V.; Pavani, M.; Catalán, M.; Maya, J. D.; Jara, J. A.; Parra, E.; Calaf, G. M.; Speisky, H.; Ferreira, J., Destabilization of mitochondrial functions as a target against breast cancer progression: Role of TPP(+)-linked-polyhydroxybenzoates. *Toxicol. Appl. Pharmacol.* **2016,** *309*, 2-14. doi: 10.1016/j.taap.2016.08.018

57. Ma, L.; Wang, X.; Li, W.; Li, T.; Xiao, S.; Lu, J.; Xu, J.; Zhao, Y., Rational design, synthesis and biological evaluation of triphenylphosphonium-ginsenoside conjugates as mitochondria-targeting anti-cancer agents. *Bioorg. Chem.* **2020,** *103*, 104150. doi: 10.1016/j.bioorg.2020.104150

58. Liou, G.-Y.; Storz, P., Reactive oxygen species in cancer. *Free Radical Res.* **2010,** *44* (5), 479-496. doi: 10.3109/10715761003667554

59. Ismail, T.; Kim, Y.; Lee, H.; Lee, D. S.; Lee, H. S., Interplay Between Mitochondrial Peroxiredoxins and ROS in Cancer Development and Progression. *Int. J. Mol. Sci.* **2019,** *20* (18), 4407. doi: 10.3390/ijms20184407

60. Sullivan, L. B.; Chandel, N. S., Mitochondrial reactive oxygen species and cancer. *Cancer Metab.* **2014,** *2* (1), 17. doi: 10.1186/2049-3002-2-17

61. Athreya, K.; Xavier, M. F., Antioxidants in the Treatment of Cancer. *Nutr. Cancer* **2017,** *69* (8), 1099-1104. doi: 10.1080/01635581.2017.1362445

62. Sayin, V. I.; Ibrahim, M. X.; Larsson, E.; Nilsson, J. A.; Lindahl, P.; Bergo, M. O., Antioxidants accelerate lung cancer progression in mice. *Sci. Transl. Med.* **2014,** *6* (221), 221ra. doi: 10.1126/scitranslmed.3007653

63. Cheng, G.; Zielonka, J.; McAllister, D. M.; Mackinnon, A. C., Jr.; Joseph, J.; Dwinell, M. B.; Kalyanaraman, B., Mitochondria-targeted vitamin E analogs inhibit breast cancer cell energy metabolism and promote cell death. *BMC Cancer* **2013,** *13*, 285. doi: 10.1186/1471-2407-13-285

64. Benfeito, S.; Fernandes, C.; Vilar, S.; Remião, F.; Uriarte, E.; Borges, F., Exploring the Multi-Target Performance of Mitochondriotropic Antioxidants against the Pivotal Alzheimer's Disease Pathophysiological Hallmarks. *Molecules* **2020,** *25* (2), 276. doi: 10.3390/molecules25020276

65. Teixeira, J.; Soares, P.; Benfeito, S.; Gaspar, A.; Garrido, J.; Murphy, M. P.; Borges, F., Rational discovery and development of a mitochondria-targeted antioxidant based on cinnamic acid scaffold. *Free Radical Res.* **2012,** *46* (5), 600-11. doi: 10.3109/10715762.2012.662593

66. Teixeira, J.; Cagide, F.; Benfeito, S.; Soares, P.; Garrido, J.; Baldeiras, I.; Ribeiro, J. A.; Pereira, C. M.; Silva, A. F.; Andrade, P. B.; Oliveira, P. J.; Borges, F., Development of a Mitochondriotropic Antioxidant Based on Caffeic Acid: Proof of Concept on Cellular and Mitochondrial Oxidative Stress Models. *J. Med. Chem.* **2017,** *60* (16), 7084-7098. doi: 10.1021/acs.jmedchem.7b00741

67. Benfeito, S.; Oliveira, C.; Fernandes, C.; Cagide, F.; Teixeira, J.; Amorim, R.; Garrido, J.; Martins, C.; Sarmento, B.; Silva, R.; Remião, F.; Uriarte, E.; Oliveira, P. J.; Borges, F., Fine-tuning the neuroprotective and blood-brain barrier permeability profile of multi-target agents designed to prevent progressive mitochondrial dysfunction. *Eur. J. Med. Chem.* **2019,** *167,* 525-545. doi: 10.1016/j.ejmech.2019.01.055

68. Kumar, P.; Nagarajan, A.; Uchil, P. D., Analysis of Cell Viability by the MTT Assay. *Cold Spring Harb. Protoc.* **2018,** *2018* (6). doi: 10.1101/pdb.prot095505

69. Moreira-Pinto, B.; Costa, L.; Felgueira, E.; Fonseca, B. M.; Rebelo, I., Low Doses of Resveratrol Protect Human Granulosa Cells from Induced-Oxidative Stress. *Antioxidants* **2021,** *10* (4). doi: 10.3390/antiox10040561

70. Borenfreund, E.; Puerner, J. A., A simple quantitative procedure using monolayer cultures for cytotoxicity assays (HTD/NR-90). *J. Tissue Cult. Methods* **1985,** *9* (1), 7-9. doi: 10.1007/BF01666038

71. Repetto, G.; del Peso, A.; Zurita, J. L., Neutral red uptake assay for the estimation of cell viability/cytotoxicity. *Nat. Protoc.* **2008,** *3* (7), 1125-1131. doi: 10.1038/nprot.2008.75

72. Kumar, P.; Nagarajan, A.; Uchil, P. D., Analysis of Cell Viability by the Lactate Dehydrogenase Assay. *Cold Spring Harb. Protoc.* **2018,** *2018* (6). doi: 10.1101/pdb.prot095497

73. Cottet-Rousselle, C.; Ronot, X.; Leverve, X.; Mayol, J.-F., Cytometric assessment of mitochondria using fluorescent probes. *Cytometry A* **2011,** *79A* (6), 405-425. doi: 10.1002/cyto.a.21061

74. Crowley, L. C.; Marfell, B. J.; Waterhouse, N. J., Analyzing Cell Death by Nuclear Staining with Hoechst 33342. *Cold Spring Harb. Protoc.* **2016,** *2016* (9). doi: 10.1101/pdb.prot087205

75. Aranda, A.; Sequedo, L.; Tolosa, L.; Quintas, G.; Burello, E.; Castell, J. V.; Gombau, L., Dichloro-dihydro-fluorescein diacetate (DCFH-DA) assay: a quantitative method for oxidative stress assessment of nanoparticle-treated cells. *Toxicol. In Vitro* **2013,** *27* (2), 954-63. doi: 10.1016/j.tiv.2013.01.016

76. Bak, M.-J.; Jeong, W.-S.; Kim, K.-B., Detoxifying effect of fermented black ginseng on H2O2-induced oxidative stress in HepG2 cells. *Int. J. Mol. Med.* **2014,** *34* (6), 1516-1522. doi: 10.3892/ijmm.2014.1972

77. Schröterová, L.; Králová, V.; Vorácová, A.; Hasková, P.; Rudolf, E.; Cervinka, M., Antiproliferative effects of selenium compounds in colon cancer cells: comparison of

different cytotoxicity assays. *Toxicol. In Vitro* **2009,** *23* (7), 1406-11. doi: 10.1016/j.tiv.2009.07.013

78. Gazzano, E.; Lazzarato, L.; Rolando, B.; Kopecka, J.; Guglielmo, S.; Costamagna, C.; Chegaev, K.; Riganti, C., Mitochondrial Delivery of Phenol Substructure Triggers Mitochondrial Depolarization and Apoptosis of Cancer Cells. *Front. Pharmacol.* **2018,** *9*, 580. doi: 10.3389/fphar.2018.00580

79. Han, M.; Vakili, M. R.; Soleymani Abyaneh, H.; Molavi, O.; Lai, R.; Lavasanifar, A., Mitochondrial Delivery of Doxorubicin via Triphenylphosphine Modification for Overcoming Drug Resistance in MDA-MB-435/DOX Cells. *Mol. Pharmaceutics* **2014,** *11* (8), 2640-2649. doi: 10.1021/mp500038g

80. Millard, M.; Gallagher, J. D.; Olenyuk, B. Z.; Neamati, N., A Selective Mitochondrial-Targeted Chlorambucil with Remarkable Cytotoxicity in Breast and Pancreatic Cancers. *J. Med. Chem.* **2013**, 56 (22), 9170-9179. doi: 10.1021/jm4012438